INCREASING CLOUD IN A WARMING WORLD

A. HENDERSON-SELLERS
Department of Geography, University of Liverpool, P.O. Box 147, Liverpool, U.K.

Abstract. Cloud amount records for the U.S.A. have been analyzed in the context of the 'warming world' analogue model described by Lough *et al.* (1983). Cloud amount increases over practically the entire U.S.A. in all seasons. This result considerably strengthens the more tentative conclusion of Henderson-Sellers (1986) that cloud amount increases over Europe in the same warming world scenario. These results are in contrast to the few numerical model predictions of cloud changes in warming world experiments. A possible, rather tantalizing, conclusion is that current GCM cloud prediction schemes tend to enhance temperature increases through cloud-climate feedback whereas the historical data could suggest a negative feedback. Part, possibly all, of this difference may be the result of the fundamental distinction between the two experimental scenarios: the equilibrium change modelled by GCMs as compared to the smaller transient change represented by the historical analogue. On the other hand the current 'real-world' experiment is, itself, a transient change in boundary and atmospheric conditions. At the least, surface-observed cloudiness seems to offer a useful and complementary data source with which to examine one aspect of the performance of numerical climate models.

1. Clouds in a Warmer World

It seems likely that the increase in the concentration of atmospheric carbon dioxide over pre-industrial levels caused predominantly by the combustion of fossil fuels will lead to increased temperatures (NAS, 1982). There are two different and complementary methods which can be employed in trying to understand and predict the response of the climate system to these increased temperatures. One method is the use of large numerical climate models. The other is the study of past climates. Interpretation of palaeoclimatological data can itself take a wide range of forms (cf. Schneider, 1986). One of these is the construction of historical analogue climate scenarios based on the instrumental record. Analysis of the period of the instrumental record is restricted to the last 100–150 y. A disadvantage of this instrumental scenario method is that this period offers relatively small hemispherical temperature changes compared with those expected to result ultimately (i.e. in an equilibrium change) from future increases in atmospheric carbon dioxide concentration. Thus instrumental scenarios, such as the study described here, might be taken as being indicative of changes and conditions to be anticipated during the early phase of CO_2-induced warming, and not necessarily of those of later stages when the gradual, but steady, rise in atmospheric CO_2 levels will cause the climate system to respond relatively slowly. The historical analogue method used here, which extracts a block of warm and a block of cold years from the instrumental record, may, fortuitously, incorporate important changes in oceanic and cryospheric boundary conditions.

The atmospheric carbon dioxide concentration is presently about 345 ppmv as com-

Climatic Change **9** (1986) 267–309.

pared with various estimates of the pre-industrial concentration ranging from 260 to 290 ppmv (e.g. Brewer, 1978; Chen and Millero, 1979; Wigley, 1983). Predictions of the likely atmospheric concentration of carbon dioxide for the year 2025 range from 440 to 600 ppmv, depending upon the forecast growth rate of energy used (Wigley, 1982). It is for this reason that climate modelling studies generally investigate the effect of doubling the atmospheric concentration of carbon dioxide. Such studies suggest that a doubling of atmospheric CO_2 will produce an increasing global mean temperature of 2–4 °C (Gates, 1980; NAS, 1982; WMO, 1986).

Probably the single most difficult climatic feedback process to measure and hence to model is the cloud-radiation feedback (GARP/JOC, 1978). Clouds affect both the incoming shortwave radiation, generally tending to increase the planetary albedo, and also the emitted terrestrial radiation tending to enhance the 'greenhouse effect' (Ohring and Clapp, 1980; Cess *et al.*, 1982). The question of which feature dominates probably varies as a function of cloud type, cloud height and cloud structure (e.g. Schneider, 1972; Shukla and Sud, 1981; Wetherald and Manabe, 1986). There are additional difficulties in estimating likely cloud-climate interactions in perturbed climate situations, such as the inability to establish whether an increase in cloudiness, e.g. as a result of increased temperatures and hence increased evaporation, leads to an increase in areal coverage by clouds (as in the case of increased stratiform clouds) or to increased vertical extent (as in the case of increased cumuliform clouds) with possibly even a decrease in areal extent. The semi-transparent nature of cirrus cloud and the dynamic nature of overlap of layered clouds make even simplified studies of cloud-climate interactions difficult (Stephens and Webster, 1979; Webster and Stephens, 1984).

Many of the climate model investigations of the likely impact of the increased atmospheric CO_2 have used specified cloud cover (e.g. Manabe and Wetherald, 1975; Mitchell, 1983). This is clearly an unsatisfactory state of affairs but one which can, perhaps, be viewed sympathetically in the light of the difficulties of parameterizing cloud processes successfully in climate models and particularly the dearth of adequate cloud data. The relatively few investigations that have been undertaken with models which include cloud prediction and hence cloud climate feedback find a greater climate sensitivity to doubling atmospheric CO_2 than the same models without feedback e.g. NAS (1982). Hansen *et al.* (1984) note that the physical process contributing the greatest uncertainty to their predicted climate sensitivity on a timescale of 10–100 y appears to be the cloud feedback.

Efforts are being made to improve the cloud observational data base (e.g. Stowe, 1984) but projects such as the International Satellite Cloud Climatology Project (ISCCP) (Schiffer and Rossow, 1983, 1985), even when successfully completed, will provide only a five year data set. In addition satellite-based cloud retrieval projects alone are unlikely to be able to furnish adequate information about cloud layering and cloud type, and the differences between satellite and surface based cloud observations preclude, at least at present, any hope of comparing present day satellite retrieved cloudiness estimates with earlier periods of surface based cloudiness observations (Malberg, 1973; Hughes, 1984). An alternative method of estimating the probable impact of a CO_2 induced warming is

that of the construction of warm-world analogues from historical meteorological records (e.g. Flohn, 1977; Wigley *et al.*, 1980; Kellogg and Schware, 1981; Lough *et al.*, 1983).

The transient nature of the current real-world experiment in which mankind is forcing an increase in the levels of CO_2 and other trace gases in the atmosphere (Dickinson and Cicerone, 1986) and the complexity of the cloud-radiation feedback combine to make any cloud/climate sensitivity study hazardous. The major advantage of using an historical analogue technique, as employed here, is that the climate (and cloud) change examined are transient. Also, in this study, both are monotonic. It is not at all certain that the temperature increase examined was caused by increasing atmospheric CO_2 or that the cloud increase is physically related to the temperature increase. Thus the results presented here are, at worst, a description of an observational data set which climate modellers could usefully exploit. On the other hand, they might indicate that the real-world transient experiment includes a negative feedback effect due to increasing cloud amount.

2. Analogue Model for a Warming World: the Case of the U.S.A.

The construction of analogue models with which to investigate the probable effects of increasing atmospheric CO_2 was pioneered by Flohn and Kellogg in 1977 and has been reviewed recently by Pittock and Salinger (1982). Wigley *et al.* (1980) composited data from individual years contrasting a group of warm years with a group of cold years. More recently Lough *et al.* (1983) have suggested an improvement on this basic technique. This analogue method was used successfully by Henderson-Sellers (1986) to examine the probable cloud variation associated with increasing temperatures in Europe. In this paper, this analogue study has been extended to a second case: the United States.

Lough *et al.* (1983) selected the warmest and coldest 20 yr periods from the gridded northern hemisphere temperature data produced by Jones *et al.* (1982). Only the temperature data for the period 1901–1980 inclusive were considered. In this period the warmest 20 yr period is from 1934–1953 and the coldest from 1901–1920. The northern hemisphere annual mean surface air temperature differed by 0.4 °C between these two periods. Lough *et al.* (1983) comment that comparison of these two periods as an analogue of a warming world has some significant advantages over the method of compositing groups of warmest and coldest years undertaken by e.g. Wigley *et al.* (1980) and Jäger and Kellogg (1983). Any changes in climatic parameters noted in going from the cold to the warm period are likely to be associated with the gradual warming from 1901 to 1983 and may be associated with the increase in atmospheric CO_2 during the early part of the twentieth century. Even if the gradual warming examined here is not the result of increasing atmospheric CO_2, the analogue of slowly changing boundary and temperature conditions is a useful tool with which to study the transient CO_2-induced changes predicted for the present and near future (Wigley and Schlesinger, 1985; Hansen *et al.*, 1985). The study described by Lough *et al.* (1983) was for Europe. More recently, Palutikof *et al.* (1984) have compared this European scenario with one for the same time periods for North America.

Palutikof *et al.* (1984) found that, in contrast to the European situation, almost all

of the continental United States shows temperature increases in the warmer world, the most extensive areas and temperature changes being in the summer and winter seasons. There is also a discontinuous belt of lowered temperatures around the latitude zone 50°-60° N, which varies seasonally. Palutikof *et al.* (1984) also show that sea-level pressure decreased over most of North America in the warmer world scenario. In particular, the continental United States, with which this paper is concerned, exhibits lower sea-level pressures in all seasons, the most extensive pressure decrease being in the wintertime, although even then the pressure differences rise to little greater than 1 hPa. This result is in marked contrast to the rather complex pattern of sea-level pressure change occurring over Europe in the same periods.

The temporal trend is of increasing cloud over the study period. Figure 1 compares the northern hemisphere temperature data, in the form of anomalies from a 1946–1960

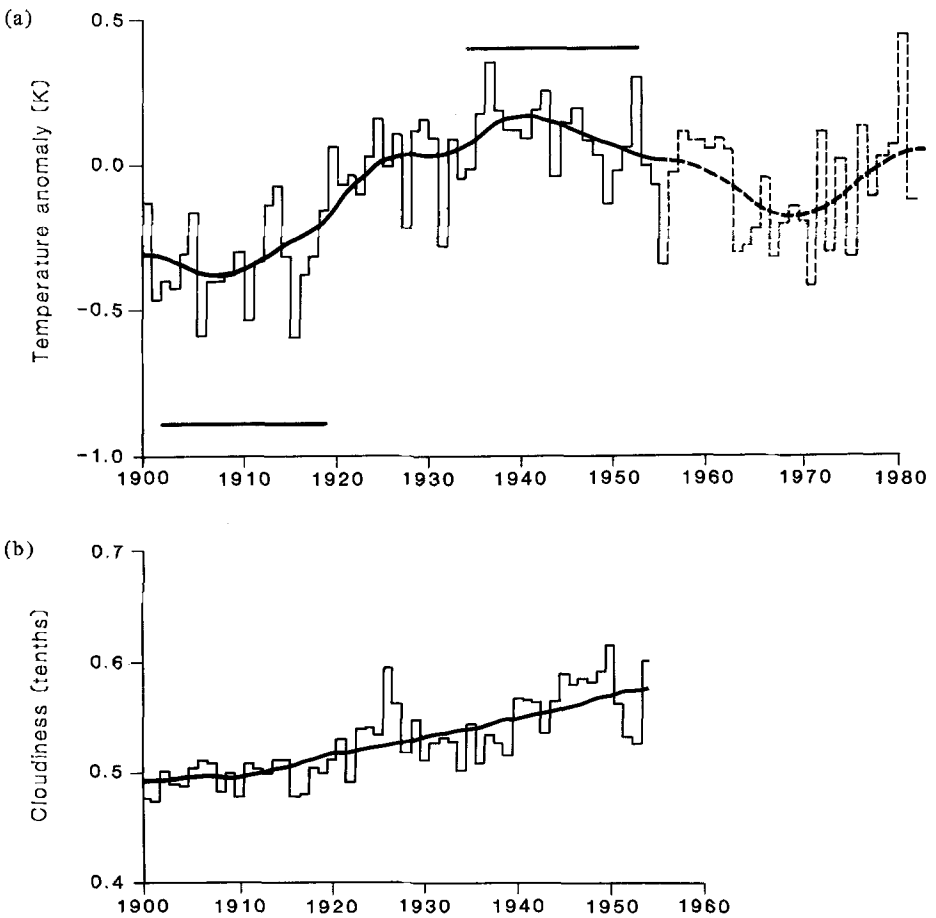

Fig. 1. (a) Northern hemisphere mean surface air temperature variations (K) since 1900 shown as anomalies from 1946–1960 reference period. The curve is of 20 yr filtered values. The warm and cold periods used here are marked (redrawn from Lough *et al.*, 1983), (b) U.S.A. mean annual cloud amount, 77 station average for the period 1900–1954. The curve is of 20 year filtered values.

reference period (Figure 1(a)) with the annual total cloud amount for the U.S.A. derived by averaging observed values from the 77 stations described below (Figure 1(b)). The gradual increase in cloud amount which is observed generally over the continental U.S.A. (e.g. Figure 2), may perhaps, be the result of the comparatively simpler sea-level pressure

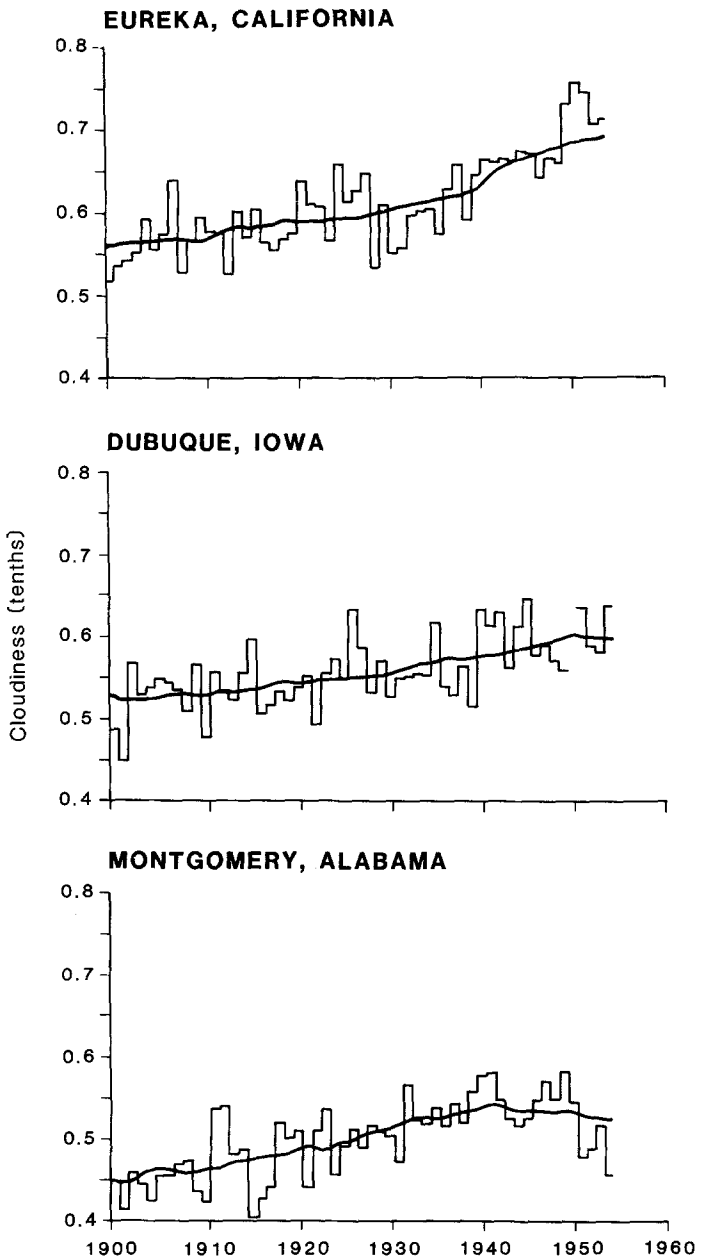

Fig. 2. Annual mean cloud amounts for Eureka, California; Dubuque, Iowa and Montgomery, Alabama. The curves are of 20 yr filtered values.

change (a general decrease) noted above. The spatially coherent upward trend in total cloud amount stengthens the case for using the historical analogue model.

Despite the monotonic trend in the temperature and total cloud amount curves shown in Figure 1, caution must be exercised when using the historical analogue method and in particular when applying it to the topic of cloud changes. The fact that hemispheric mean temperatures fell by ~0.3 °C in the 30 yr (1945–1975) when atmospheric CO_2 concentrations were increasing most rapidly suggests that factors other than CO_2, or combining with CO_2, have at least a comparable effect on temperature. Recent estimates of the increase in global mean temperature over the last century (Wigley and Schlesinger, 1985) which allow for oceanic thermal inertia range between 0.3 and 0.8 °C. Thus the contribution of increased CO_2 to the observed warming between the two twenty year periods used here is likely to be ~0.2 °C suggesting that, at most, only approximately half the observed warming of 0.4 °C can be attributed to CO_2. There is no guarantee that the other factors contributing to the observed warming, for example long term but, perhaps, eventually random fluctuations in ocean temperature (Folland *et al.*, 1984; Jones *et al.*, 1986) would produce the same changes in cloudiness found with increased CO_2. For example, with enhanced CO_2, the continents would be expected to warm faster than the oceans, whereas with a warming 'driven' by the ocean, the opposite might be true, and then the changes in cloud would be different, especially near coasts. Despite these caveats this investigation of cloud amounts offers a possible link between increasing atmospheric CO_2 and cloudiness which is an alternative to numerical modelling results. Additionally the cloud data described here offer a means of examining the predictions of numerical climate models which should be exploited (see Section 6).

3. Historical Cloud Data for the Continental U.S.A.

Cloud observations are not included in the World Weather Record and thus archive data sources must be sought if the historical record of cloud amount is to be analyzed. Some cloud data are available for the United States on computer-readable magnetic tapes at the National Center for Atmospheric Research. However, Jenne (1984, p.c.) states that no cloud data are available on tape prior to 1948 for the U.S.A. (cf. Warren *et al.*, 1985). It was therefore necessary to consult documentary records held at the National Climatic Data Center in Asheville, N.C.

As might be anticipated, quantity and areal coverage of climatic data increase with time. In this study, it was essential to obtain similar cloud information for the cold and warm periods identified: 1901–1920 and 1934–1953. Unlike the situation in Europe, where observations of a meteorological nature had often been made since the seventeenth century and were commonplace by the early 1900s at many national (often astronomical) observatories, climatic data for the early part of this century are somewhat sparce in the United States. In particular, before the advent of commercial aircraft in the 1930s, there was little requirement for continuous weather observations and consequently relatively few were made. Of course there are exceptions to this, but these tend to be in locations on the eastern seaboard in centres of early settlement.

There were three possibile sources from which cloud information could have been drawn. The U.S. Daily Weather Maps are available on microfilm for the period 1900–1921 and 1933–1954. There is one map per day and the cloud information is quite sketchy, particularly in the early period with the station circle indicating only clear, partly cloudy or overcast conditions, although by the early 1940s, the modern depiction of cloud cover and type is adopted. Another choice is the Weather Bureau Form 1001. This is a monthly record of observations which includes cloud type, amount and movement. However, these cloud observations are made at only one time in each day. The final data source, and the one which was selected here, was the Climatological Record Book. This data archive contains records from many reporting stations, often with long and continuous periods of observation. It includes cloud data which are in monthly averaged form for two or more observation times per day. This latter archive source, which is available on 35 mm microfilm at the National Climatic Data Center, seemed to be the most appropriate in that it offered the best chance of obtaining good spatial coverage for the continental U.S.A. within the constraint of the temporal coverage required, which must include the cold and warm periods essential for this analogue model study.

The periods spanned by the four volumes of the Climatological Record Book are 1871–1910, 1911–1930, 1931–1950, and 1951–1970. In order to obtain data for the period 1900–1954 (which is necessary to permit filtering of the two 20 yr time periods studied here), all 4 volumes had to be consulted. The Climatological Record Book contains two cloud observations under the sub-heading 'weather', the first being average cloudiness and the second the number of days which have been clear, partly cloudy or cloudy. It was the first of these data sets which was used here.

It is necessary in a study such as this to obtain as good and consistent a spatial coverage as possible. A pre-selection was made of the stations which possessed continuous meteorological records in the archive, but after consultation of the records themselves it was necessary to modify the station list quite considerably. Finally it was possible to find 77 stations for which a complete, or near complete, cloud record was available for the period 1900–1954. These stations are listed in Table I, which also notes their location and some geographic and topographic details. The difficulties described in Henderson-Sellers (1986) of relocation of stations appear to be very much worse in the U.S.A. than in Europe with up to 10 relocations in one case (Table I). On the other hand these station moves were often only a few tens of metres or less. Clearly considerable care has been taken in this station relocation and it is rare for the record (at least of clouds) to be badly disturbed by these changes. However, these small changes must be added to the other inevitable disturbances due to urbanisation and alteration of the station environment which has occurred in very many locations. In view of these difficulties, a decision was made that no alternative (i.e. spatially separate) station should be used to substitute for any gaps in the cloud record of the U.S.A. stations.

In addition to these difficulties, there have been changes in observing practice through time. These are fortunately not as dramatic as in Europe, but may still cause discontinuities in the historical record. There are usually only two observations each day during

TABLE I: List of stations including last location, number of locations, geographic and topographic information and notes on observation times.

Station	Latitude (N)	Longitude (W)	Ht(m) & [no. of locations]	Location description	Observation times
Mobile, Alabama	30°41′	88°15′	63 [6]	At head of Mobile Bay very much influenced by the Gulf of Mexico 48 km away	7 am & 7 pm 1900–1930 7 am, noon, 7 pm 1931–1939 7 am & 7 pm July 1939–Dec 1941 Monthly avs 1942–1950 0000, 0600, 1200 & 1800 1951–1954
Montgomery, Alabama	32°18′	86°24′	59 [5]	Located in a gently rolling area, no real topographic features which influence weather and climate. Airport terrain is level with long gentle slopes to the North-East and East [Danelly Field].	7 am & 7 pm 1900–1930 7 am, noon, 7 pm 1931– April 1943 Monthly avs 1944–1950 May 1944–Dec 1950 0000, 0600, 1200 & 1800 1951–1954
Fort Smith, Arkansas	35°20′	94°23′	137 [4]	Located at the confluence of the Potean & Arkansas Rivers. Terrain influences weather. 32 km to the west are the Cookson Hills (rising to 450 m) and the same distance to the North-East are the Boston Mountains rising to 810 m.	7 am & 7 pm 1900–1930 7 am, noon, 7 pm 1931–1942 Monthly avs 1944–1950 0300, 0630, 1230 & 1830 1951–1954
Phoenix, Arizona	33°26′	112°01′	334 [9]	Phoenix situated in the centre of the Salt River Valley; nearly flat plain. Southern Mountains rising to 780 m are 9.6 km to South and 13 km to the North are the Phoenix mountains which rise to 810 m.	5.32 am & 5.32 pm 1900–1910 6 am & 6 pm 1911–1930 6 am, noon & 6 pm 1930–1941 Monthly avs 1944–1948 0530, 11.30, 17.30 & 23.30 1951–1954
Eureka, California	40°48′	124°10′	13 [2]	There are no hills of any consequence; Humboldt Bay is 0.4 km to North and 1.6 km to the West. The coastal range which begins 4.8 km to East of the station has an average elevation of 600 m.	8 am & 8 pm 1900–1930 5 am, Noon & 5 pm 1931–1936 4.30 am, Noon & 4.30 pm 1937–June 1939 10.30 am, Noon & 10.30 pm July 1939–1942 Av. daily cloudiness, sunrise to sunset 1943–1954

Table I: (continued)

Station	Latitude (N)	Longitude (W)	Ht(m) & [no. of locations]	Location description	Observation times
Los Angeles, California	33°56′	118°23′	29 [9]	Pacific is primary moderating influence. Coastal mountains which lie along the North and East sides of the L.A. coastal basin act as buffer against extremes.	5 am & 5 pm 1900–1930 5 am, Noon, 5 pm 1931–April 1944 Monthly avs May 1944–1948 0430, 1030, 1630 & 2230 1951–1954
San Diego California	32°44′	117°10′	4 [4]	Located on San Diego Bay on the SW corner of S. California. Influenced by the Pacific and by coastal valleys and foothills	5 am & 5 pm 1900–1930 5 am, Noon & 5 pm 1931–1936 4.30 am, Noon & 4.30 pm 1937–1939 4.30 am, 4.30 pm July 1939–1941 Monthly av. cloudiness, sunrise to sunset Jan. 1942–~1943 4.30 am, 10.30 am, 4.30 pm & 10.30 p, 1951–1954
San Francisco California	37°37′	122°23′	0.3 [5]	Situated on a flat, filled tideland of San Francisco Bay. San Brund Mountains rising to 390 m are 8 km to NNW.	8 am & 8 pm 1900–1930 8 am, noon and 8 pm 1931–1941 0430, 1030, 1630 & 2230 1942–1954
Pueblo, Colorado	38°17′	104°31′	1405 [4]	Located inland at junction of Arkansas and Fountain rivers. Mountains 40 km to the SW and 56 km to the NW. The terrain of airport is flat at about 150–210 m above the river.	6 am & 6 pm 1900–1930 6 am, noon & 6 pm 1931–1941 Av. cloudiness sunrise to sunset 1942–1950 0530, 1130, 1730 & 2330 1951–1954
New Haven, Connecticut	41°16′	72°42′	NO DATA [4]	Long Island is 1 km from this site and to the East is flat airport site.	8 am & 8 pm 1900–1930 7.45 am & 7.45 pm 1931–1936 7.15 am & 7.15 pm 1937–1942 Monthly average cloudiness 1943–1950
Washington, D.C.	38°51′	77°03′	4 [5]	Located at Western edge of the middle Atlantic Coastal Plain about 80 km East of the Blue Ridge Mountains	8 am & 8 pm 1900–1930 8 am, noon & 8 pm 1931–1941 8 am & 8 pm 1942

Table I: (continued)

Station	Latitude (N)	Longitude (W)	Ht(m) & [no. of locations]	Location description	Observation times
					Mean daily cloudiness sunrise to sunset from Jan 1951–Sept 1953
Jacksonville, Florida	30°25′	81°39′	7 [6]	Located 64 km inland; the surrounding terrain is level. Easterly winds from the ocean are a moderating influence.	7 am & 7 pm 1900–1930 8 am, noon & 8 pm 1931–June 1939 8 am & 8 pm July 1939–end of 1943 Monthy avs 1944–1950 0130, 0730, 1330, 1930 1951–1954
Key West, Florida	24°35′	81°42′	2 [9]	Located at the West end of Florida keys which are a chain of islands SW from the SE coast of the Florida peninsula. Their maximum elevation is 6 m; mean elevation is 2.4 m.	7 am & 7 pm 1900–1930 8 am, noon & 8 pm 1931–June 1939 8 am & 8 pm July 1939–end 1941 Av. cloudiness, sunrise to sunset 1942–1950 0100, 0700, 1300, 1900, 1951–July 1954 0700, 1300, 1900 Aug. 1954–end 1954
Pensacola, Florida	30°28′	87°12′	34 [4]	Situated on a hilly, sandy slope bordering Pensacola Bay, 10 km from Gulf of Mexico	7 am 1900–1911 7 am & 7 pm 1911–1930 Monthly mean cloudiness 1931–1950 Sky cover - monthly av. (sunrise to sunset) 1951–1954
Tampa, Florida	27°58′	82°32′	6 [5]	Flat Terrain with influence of the Gulf of Mexico and bays	7 am & 7 pm 1910 8 am & 8 pm 1911–1930 8 am, noon & 8 pm 1931–Dec 1936 7.10 am, noon & 7.10 pm Jan 1937–end 1941 Av. cloudiness, sunrise to sunset 1944–1948 1.30 am, 7.30 am, 1.30 pm, 7.30 pm 1951–1954
Macon, Georgia	32°42′	83°39′	107 [7]	Flat terrain, to the west a range of wooded hills [nearest point is 4 km away]	7 am 1900–April 1912 8 am & 8 pm May 1912–1930

Table I: (continued)

Station	Latitude (N)	Longitude (W)	Ht(m) & [no. of locations]	Location description	Observation times
				which rise to 90 m.	Monthly av. cloudiness sunrise to sunset 1931–1950 1.30, 7.30, 13.30, 19.30 1951–1954.
Des Moines, Iowa	41°32′	93°39′	284 [5]	Situated in a gently rolling plain which has little effect on the weather.	7 am & 7 pm 1900–1930 Av. monthly cloudiness 1931–1950 00,06, 12 & 1800 hrs. 1951–1954.
Dubuque, Iowa	42°24′	90°42′	320 [4]	Terrain varies from gently rolling at 16–24 km distance, to steep hills and bluffs to the West around the city.	7 am & 7pm 1900–1930 7 am, noon & 7 pm 1931–Jan 1944 Av. cloudiness Feb 1944–end 1948 0000, 0600, 1200, 1800 Febr 1951–Dec 1957 0600, 1200, 1800, 1952–1954.
Boise, Idaho	43°34′	116°13′	852 [4]	Situated in a river valley, 13 km from the mouth of Mount Canyon where valley begins. Average height is 813 m.	8 am & 8 pm 1900–1910 6 am & 6 pm 1911–1930 6 am, noon & 6 pm (Noon=11.30 am from 7/1/39) 1931–1941 0530, 1130, 1730, 2330 1951–1954.
Chicago, Illinois	41°47′	87°45′	183 [4]	Situated on the SW shore of Lake Michigan and occupies a plain which is mostly only a few metres above the lake. Topography does not significantly affect air flow.	7 am & 7 pm 1900–1930 7 am, noon & 7 pm 1931–1936 6.30 am, noon & 6.30 pm 1937–1941 Av. cloudiness, sunrise to sunset 1944–1950 0030, 0630, 1230 & 1830 1951–1954.
Peoria, Illinois	40°40′	89°41′	196 [4]	Airport station on rather level tableland surrounded by well drained and gently rolling terrain.	7 am & 7 pm 1905 (only am for 1905)–1930 7 am, noon & 7 pm 1931–1941 Av. cloudiness, sunrise to sunset, 1942–1950 0030, 0630, 1230, 1830 1951–July 1953 0630, 1230, 1830 Aug 1953–Dec 1954.
Evansville, Indiana	38°03′	87°32′	115 [6]	Located on the Ohio River. Terrain	7 am 1900–1910

Table I: (continued)

Station	Latitude (N)	Longitude (W)	Ht(m) & [no. of locations]	Location description	Observation times
				ranges from level to areas of rolling ground. Dress Regional airport is located in a shallow valley with low hills to the East and West.	8 am & 8 pm 1911–1930 8 am, noon & 8 pm 1931–1941 Monthly av. clouds, sunrise to sunset 1944–1950 0030, 0630, 1230 & 1830 1951–1954.
Indianapolis, Indiana	39°44′	86°16′	238 [5]	Situated on level, slightly rolling terrain. Most of the city lies on the East of the White River which flows North to South.	7 am & 7 pm 1900–1917 7 am, noon & 7 pm 1918–1939 Av. cloudiness, sunrise to sunset 1943–1950 0000, 0600, 1200, 1800 1951–1954.
Dodge City, Kansas	37°46′	99°58′	778 [5]	Situated 480 km east of the Rockies.	7 am & 7 pm 1900–1910 8 am & 8 pm 1911–1930 7 am, noon & 7 pm 1931–1941 Mean daily cloudiness 1942–1950 12.30 am, 6.30 am, 12.30 pm & 6.30 pm 1951–1954.
Lexington, Kentucky	38°02′	84°36′	294 [4]	Fayette County, of which Lexington is the county seat, is a gently rolling plateau with an elevation of 270 to 315 m above mean sea level.	Monthly Cloudiness 1900–1930 7 am, noon & 7 pm 1931–1932 Monthly av. cloudiness, sunrise to sunset 1933–1950 12.20 am, 6.20 am, 12.20 pm & 6.20 pm 1951–1954.
Shreveport, Louisiana	32°28′	93°49′	76 [7]	Located on the West side of the Red River. The airport is 11 km SW of downtown.	7 am & 7 pm 1900–1910 8 am & 8 pm 1911–1930 Monthly av. cloudiness, sunrise to sunset 1931–1950 12.15 am, 06.15 am, 12.15 pm, 6.15 pm 1951–1954.

Table I: (continued)

Station	Latitude (N)	Longitude (W)	Ht(m) & [no. of locations]	Location description	Observation times
Nantucket, Massachusetts	~41°16′	~70°12′	NO DATA [3]	An island near Cape Cod. Terrain is level, with few low hills. The South shore of the island is about 2 km from the station.	8 am & 8 pm 1900–1930 8 am, noon & 8 pm 1931–1941 Monthly av. cloudiness, sunrise to sunset 1942–1950 0130, 0730, 1330, 1930 1951–1954.B
Baltimore, Maryland	39°11′	76°40′	44 [3]	Adjacent to Chesapeake Bay, the Atlantic Ocean is to the East, the Appalachians to the West.	Av. Monthly cloudiness 1900–1930 8 am, noon & 8pm 1931–1944 8 am & 8 pm 1945–1948 0100, 0700, 1300, 1900 1951–1954.
Eastport, Maine	~44°55′	~66°57′	NO DATA [no data]	On the Western shore of a harbour opening onto the Bay of Fundy. Nearby hills rise to 90 m. The station is less than 30 m above high water mark.	8 am & 8 pm 1900–1930 Av. mean cloudiness, sunrise to sunset 1931–1950.
Detroit, Michigan	42°14′	83°32′	217 [4]	Near the centre of Detroit's urban area, until 1966 when moved to the Metropolitan Airport in the far SW suburbs. Nearly flat land ~16 km from W. end of Lake Erie.	7 am & 7 pm 1900–1930 8 am & 8 pm July 1939–1948 8 am & 8 pm July 1939–1948 1 am, 7 am, 1 pm & 7 pm 1951–1954.
Marquette, Michigan	46°32′	87°33′	424 [3]	Airport lies approx. 12 km SW of the nearest shoreline of Lake Superior and 13 km West of the City of Marquette.	7 am & 7 pm 1900–1910 8 am & 8 pm 1911–1930 7 am, noon & 7 pm 1931–1941 Monthly av. cloudiness 1942–1950 7.30 am, 1.30 pm, 7.30 am & 1.30 pm 1951–1954.
Sault Ste. Marie, Michigan	46°28′	84°22′	216 [4]	Located at extreme tip of Michigan Upper Peninsula at the "hub" of Lakes Superior. Michigan, Huron. Terrain is mostly flat ~230 m above sea level.	7 am & 7 pm 1900–1930 Average cloudiness, sunrise to sunset 1931–1950 1 am, 7 am, 1 pm, 7 pm 1951–1954.

Table I: (continued)

Station	Latitude (N)	Longitude (W)	Ht(m) & [no. of locations]	Location description	Observation times
Columbia, Missouri	38°58′	92°22′	233 [5]	Located a little to the north of the centre of the state, 16 km NE of the Missouri River. Surrounding terrain is rolling.	7 pm 1900–1911 Monthly av. 1911–1916 Noon in 1917 7 am & 7 pm 1918–1930 7 am & noon 1931–1939 Mean daily cloudiness 1940–1950.
St. Louis, Missouri	38°45′	90°23′	166 [7]	Located at the confluence of the Missouri and Mississippi Rivers and near the geographical centre of the USA.	8 am & 8 pm 1900–1930 7 am, noon & 7 pm 1931–1941 Sunrise to sunset, monthly cloudiness 1944–1950 Midnight, 6 am, noon and 6 pm 1951–1954.
Vicksburg, Mississippi	32°21′	90°53′	70 [3]	Located on a bluff overlooking the Mississippi River which flows S., West of the City.	8 am & 8 pm 1900–1910 7 am & 7 pm 1911–1930 7 am, noon & 7 pm 1931–June 1939 7 am & 7 pm July 1939–1941 Mean daily cloudiness, sunrise to sunset 1944–1950 Average sky cover sunrise to sunset 1951–1954.
Havre, Montana	48°34′	109°40′	746 [2]	Situated in a level valley formed by the Milk River (flows W to E). The Bearpaw Mountains extend 24 to 48 km South of Havre rising to 1500 m.	6 am & 6 pm 1900–1930 6 am, noon & 6 pm 1931–1942 5.30 am, noon & 5.30 pm 1937–1942 Average cloudiness, sunrise to sunset 1944–1950 Mean monthly cloudiness 1951–1954.
Kalispell, Montana	48°18′	114°16′	890 [4]	Influenced by surrounding topography. High mountains to the East which rise to 1350 m above valley floor.	6 am & 6 pm 1900–1930 6 am, noon & 6 pm 1931–Jan 1942 5.30 am, 11.30 am, 5.30 pm & 11.30 pm 1951–1954.

Table I: (continued)

Station	Latitude (N)	Longitude (W)	Ht(m) & [no. of locations]	Location description	Observation times
Charlotte, North Carolina	35°13′	80°56′	218 [10]	Located in the S. Piedmont region. Mountains extend from SW to NE being 130–140 km from Charlotte on the W. and N. General elevation is 219 m.	8 am & 8 pm 1900–1930 Average monthly cloudiness (daylight hours) 1931–1950 1 am, 7 am, 1 pm and 7 pm 1951–1954.
Hatteras, North Carolina	35°13′	75°41′	NO DATA [3]	The terrain to the NW and NE is sandy, whilst on the SW and SE is marsh and creeks. Atlantic Ocean is 2 km to SE.	Monthly cloudiness 1903–1912 8 am & 8 pm 1913–1930 8 am, noon & 8 pm 1931–June 1939 8 am & 8 pm July 1939–1941 Average cloudiness 1942–1950 1.30 am, 7.30 am, 1.30 pm & 7.30 pm 1951–1954.
Fargo, North Dakota	46°54′	96°48′	268 [5]	Surrounding terrain is flat. The Red River Valley lies 3 km to the East.	8 am & 8 pm 1900–1910 7 am & 7 pm 1911–1930 7 am, noon & 7 pm 1931–1945 Mean cloudiness, sunrise to sunset 1946–1950 12.30 am, 6.30 am, 12.30 pm & 6.30 pm 1951–1954.
Williston, North Dakota	48°09′	103°37′	563 [4]	Lies in a flat valley at the junction of the Missouri River and Little Muddy Creek. Hills 10 km to the E rise to 90 m.	7 am & 7 pm 1900–1930 7 am, noon & 7 pm 1931–1941 Av. cloudiness, sunrise to sunset 1942–1950 0030, 0630, 1230 & 1830 1951–1954 0630, 1230, 1830 for June, July, Aug, Sept & Oct 1954.
Lincoln, Nebraska	40°51′	96°46′	352 [10]	Surrounding country is gently rolling prairie. The W. edge of the city is in the flat valley of Salt Creek.	7 am & 7 pm 1900–1930 Mean daily cloudiness, sunrise to sunset 1931–1950 12.30 am, 6.30 am, 12.30 pm & 6.30 pm 1951–1954.

Table I: (continued)

Station	Latitude (N)	Longitude (W)	Ht(m) & [no. of locations]	Location description	Observation times
North Platte, Nebraska	41°08′	100°41′	834 [6]	Located in valley. Hills are 100–150 m high.	7 am & 7 pm 1900–1930 7 am, noon & 7 pm 1931–1944 Monthly cloudiness sunrise to sunset 1944–1950 12.30 am, 6.30 am, 12.30 pm & 6.30 om 1951–1954.
Atlantic City, New Jersey	39°27′	74°35′	18 [3]	The city office is 16 km WNW of Atlantic City and the Atlantic Ocean. The terrain is flat with an elevation of ~15 m.	8 am & 8 pm 1900–1930 8 am, noon & 8 pm 1931–Jan 1944 Average cloudiness, sunrise to sunset Feb 1944–1950 7.30 am, 1.30 pm & 7.30 pm 1951–1954.
Roswell, New Mexico	33°24′	104°32′	1084 [4]	Higher land masses surround the valley location with long gradual descent from points SW through W & N.	6 am & 6 pm 1905–1930 6 am, noon & 6 pm 1931–1941 5 am, 11 am, 5 pm & 11 pm 1951–1954.
Reno, Nevada	39°30′	119°47′	1319 [5]	Situated on a semi-arid plateau in the lee of the Sierra Nevada mountains, which rise to 3300 m.	5 am & 5 pm 1906–1930 5 am, noon & 5 pm 1931–1939 Average monthly cloudiness, sunrise to sunset 1944–1950 4.30 am, 10.30 am, 4.30 pm & 10.30 pm 1951–1954.
Winnemucca, Nevada	40°54′	117°48′	1290 [4]	Cut off from the Pacific by the Sierra Nevada and situated on a plateau.	5 am & 5 pm 1900–1930 5 am, noon & 5 pm 1931–1936 4.30 am, noon & 4.30 pm 1937–June 1939 10.30 am, noon & 1.30 pm July 1939–Jan 1944 Av. monthly cloudiness, sunrise to sunset Feb 1944–1950 0410, 1010, 1610 & 2210 1951–1954.

Table I: (continued)

Station	Latitude (N)	Longitude (W)	Ht(m) & [no. of locations]	Location description	Observation times
Binghamton, New York	42°13′	75°59′	480 [6]	Situated in south central, New York State. Binghamton lies in a narrow valley at the confluence of Susquehanna and Chenago Rivers. Surrounding hills	Daylight cloudiness 1900–1930 8 am, noon & 8 pm 1931–Feb 1942 Daylight Cloudiness March 1942–1950 1.30 am, 7.30 am, 1.30 pm & 7.30 pm 1951–1954.
Rochester, New York	43°07′	77°40′	163 [4]	Located at the mouth of River Genesee, at the mid-point of the Southern shore of Lake Ontario. Land slopes from lake shore elevation of 74 m to over 300 m within 32 km.	8 am & 8 pm 1900–1930 8 am, noon & 8 pm 1931–Aug 1938 8 am & 8 pm Sept 1938–June 1948 1.30 am, 7.30 am, 1.30 pm, 7.30 pm 1951–1954.
Columbus, Ohio	40°00′	82°53′	245 [5]	Situated at the centre of the state, in drainage area of Ohio River. The elev., of the airport is 244 m above sea level.	7 am & 7 pm 1900–1930 8 am, noon & 8 pm 1931–June 1939 1.30, 7.30, 1330, 1930 1951–1954.
Toledo, Ohio	41°34′	83°28′	187 [5]	Situated at the West end of Lake Erie at the mouth of the Maumee River. Terrain is generally level with a slight slope towards the river and Lake Erie.	7 am & 7 pm 1900–1930 Cloudiness av. Daylight 1931–1950 0130, 0730, 1330, 1930 1951–1954.
Oklahoma City, Oklahoma	35°24′	97°36′	384 [5]	Located along the N. Canadian River. Surrounding country is gently rolling with nearest mountains 128 km to the South.	8 am & 8 pm 1900–1910 7 am & 7 pm 1911–1930 7 am, noon & 7 pm 1931–1943 Av. monthly cloudiness, sunrise to sunset 1944–1950 0000, 0600, 1200, 1800 1951–1954.
Portland, Oregon	45°36′	122°36′	6 [11]	The office is 10 km NNE of downtown Portland; the latter is 104 km inland from the Pacific Ocean. The nearby steep slope of the Columbia range creates orographic uplift.	8 am & 8 pm 1900–1910 5 am & 5 pm 1911–1930 5 am, noon & 5 pm 1931–Sept 1942 Av. cloudiness sunrise to sunset October 1942–1950

Table I: (continued)

Station	Latitude (N)	Longitude (W)	Ht(m) & [no. of locations]	Location description	Observation times
					0400, 1000, 1600 & 2200 1951–1954.
Roseburg, Oregon	43°13′	123°20′	152 [4]	Lies in a narrow river valley, surrounded by wooded rolling hills, (210–270m in elevation) within 2 km of station.	5 am & 5 pm 1900–1930 5 am, noon & 5 pm 1931–June 1939 5 am & 5 pm July 1939–1941 Monthly av. cloudiness 1944–1950 10.30 am & 4.30 pm 1951–1954.
Erie, Pennsylvania	42°05′	80°05′	220 [4]	Located on the South-east shore of Lake Erie; terrain rises gradually in a series of ridges paralleling the shoreline to 150 m above lake level.	8 am & 8 pm 1900-1930 8 am, noon & 8 pm 1931–Jan 1944 Av. monthly cloudiness, sunrise to sunset February 1944–1950 Av. monthly skycover 1951–Aug 1954.
Philadelphia, Pennsylvania	39°53′	75°15′	4 [6]	The Appalachians are to the West, and the Atlantic Ocean is to the East. Terrain is flat with the Delaware River immediately East.	8 am & 8 pm 1900–1930 Av. Daily cloudiness 1931–1950 1.30 am, 7.30 am, 1.30 pm & 7.30 pm 1951–1954.
Block Island, Rhode Island	41°10′	71°35′	33 [4]	Block Island Station is 0.2 km ENE of Long island and 19 km South of Charleston, Rhode Island.	8 am & 8 pm 1900–1930 Monthly av. cloudiness 1931–1950 0730 & 1330 1951–1954.
Charleston, South Carolina	32°54′	80°02′	12 [5]	Situated on a peninsula bounded on the W. and S. by the Ashley River, on the E. by Cooper River and on the SE by a harbour. Terrain is generally level ranging in elevation from sea level to 6 m.	8 am & 8 pm 1900–1930 monthly cloudiness 1931–1950 0130, 0730, 1330, 1930 1951–1954
Columbia, South Carolina	33°57′	81°07′	65 [9]	Centrally located in the state. It lies on Congoree River near the confluence of the Broad & Saluden Rivers. Terrain is rolling, sloping from 105 m to 60 m above sea level.	8 am & 8 pm 1900–1930 8 am, noon & 8 pm 1931–Febr 1942 Av. cloudiness, sunrise to sunset 1944–1950.

Table I: (continued)

Station	Latitude (N)	Longitude (W)	Ht(m) & [no. of locations]	Location description	Observation times
Huron, South Dakota,	44°23′	98°13′	385 [3]	Located on the West Bank of James River at the middle of the river valley. Terrain is very flat and level.	7 am & 7 pm 1900–1930 7 am, noon & 7 pm 1931–1948 0030, 0630, 1230, 1830 1951–1954.
Knoxville, Tennessee	35°49′	83°59′	285 [6]	Located in a broad valley between the Cumberland Mountains which lie NW of City and the Great Smoky Mountains which lie SE of the city.	7 am & 7pm 1900–1930 7 am, noon & 7 pm 1931–1943 Av. daily cloudiness, sunrise to sunset 1944–1950 0130, 0730, 1330 & 1930 1951–1954.
Amarillo, Texas	35°14′	101°42′	1077 [6]	A region of flat topography. Canadian River flows East, 29 km N. of station with its bed about 240 m below the plains.	7 am & 7 pm 1900–1930 7 am, noon & 7 pm 1931–1950 12.30 am, 6.30 am, 12.30 pm, 6.30 pm 1951–1954.
Corpus Christi, Texas	27°46′	97°27′	12 [7]	Located on Corpus Christi Bay, an inlet of the Gulf of Mexico. The airport is 11 km west of downtown Corpus Christi.	7 am & 7 pm 1900–1930 7 am, noon & 7 pm 1931–1941 Av. skycover, sunrise to sunset 1942–1950 0030, 0630, 1230 & 1830 1951–1954.
Galveston, Texas,	29°18′	94°48′	2 [3]	Situated on Galveston Island of the SE coast of Texas. The island is 4.4 km across at its widest point and 46.4 km long.	7 am & 7 pm 1900–1930 7 am, noon & 7 pm 1931–1942 Mean cloudiness, sunrise to sunset 1943–1950.
San Antonio, Texas	29°32′	98°28′	238 [8]	Situated in the S. Central part of Texas; to the NW of the city the terrain slopes upward to Edwards plateau and to SE, slopes down to Gulf coastal plains.	Not recorded from 1900–1910 7 am & 7 pm 1911–1930 7 am, noon & 7 pm 1931-1943 Sunrise to sunset av. cloudiness 1944–1950 0030, 0630, 1230, 1830 1951–1954.
Salt Lake City, Utah	40°46′	111°58′	1266 [6]	Situated in the North of Utah on the Western slope of the Wasatch Mountains,	6 am & 6 pm 1900–1930 6 am, noon & 6 pm 1931–1950

Table I: (continued)

Station	Latitude (N)	Longitude (W)	Ht(m) & [no. of locations]	Local description	Observation times
				rising to elevations of 3600 m. Close to the Great Salt Lake, the Oquirrh Mountains are 32 km to the SW, several peaks of which are above 3000 m.	0530, 1130, 1730 & 2330 1951–1954.
Norfolk, Virginia	36°53′	76°12′	8 [6]	Surrounded by water, with Chesapeake Bay to the North and Atlantic Ocean 29 km away to the East. Av. elevation is ~4 metres; the land is low and level with no nearby hills.	8 am & 8 pm 1900–1930 8 am, noon & 8 pm 1931–1941 Mean monthly cloudiness 1944–1950 0130, 0730, 1330, 1930 1951–1954.
Richmond, Virginia	37°30′	77°20′	49 [8]	Situated in east-central Virginia at the head of navigation on the James River. Blue Ridge Mountains lie about 144 km to the West, and Chesapeake Bay is 96 km to the East. Elevations range from sea level to 480 m in the West.	8 am & 8 pm 1900–1910 – averaged 8 am & 8 pm 1911–1930 8 am, noon & 8 pm 1931–1943 Av. cloudiness 1944–1950 0100, 0700, 1300 & 1900 1951–1954.
Burlington, Vermont	44°28′	73°09′	99 [4]	Located on the E. shore of Lake Champlain at the widest part of the lake. 56 km to the West lie the highest of the Adirondack Mts.	Av. monthly cloudiness 1906–1910 8 am 1911–1930 Av. monthly cloudiness 1931–1950 0130, 0730, 1330, 1930 1951–1954.
Seattle, Washington	47°36′	122°20′	4 [4]	Located on a hilly stretch of land overlooking the salt waters of Puget Sound to the West. Hills rise abruptly on both sides, up to elevations of 90 m.	5 am & 5 pm 1900–1930 Av. cloudiness, sunrise to sunset 1931–1950 0430, 1030, 1630, 2230 1951–1954.
Spokane, Washington	47°37′	117°31′	707 [5]	Lies on the eastern edge of Columbia basin. Elevations in E. Washington vary from less than 120 m above sea level near Pasco, to over 1500 m in the E. extremes of the state.	5 am & 5 pm 1900–1930 5 am, noon & 5 pm 1931–1943 Av. cloudiness 1944–1950 0430, 1030, 1630 & 2230 1951–1954.

Table I: (continued)

Station	Latitude (N)	Longitude (W)	Ht(m) & [no. of locations]	Local description	Observation times
Walla Walla, Washington	46°02′	118°20′	285 [4]	Located near the upper end of a wide valley which extends from the main valley of the Columbia River. The Blue Mountains rise to the S, SE, and East of the city, with foothills 16 km away. There are rolling hills with elevations up to 600 m to the North and North East.	8 am & 8 pm 1900–1910 5 am & 5 pm 1911–1930 5 am, noon & 5 pm 1931–1940 (Noon obs., discontinued July 1, 1939) Av. cloudiness sunrise to sunset 1941–1950 10.30 am 1951–1954.
Milwaukee, Wisconsin	42°57′	87°54′	202 [4]	Situated on the West coast of Lake Michigan.	7 am & 7 pm 1900–1930 Monthly mean cloudiness, daylight hours 1931–1950 0000, 0600, 1200, 1800 1951–1954.
Elkins, West Virginia	38°53′	79°51′	591 [4]	The airport and city are located near the middle of a valley, with ridges at or near 1000 m. Valley is located on the North West slope of the Appalachians which rise to 1350 m 32 km to the SE.	8 am & 8 pm 1900–1930 Monthly mean cloudiness, sunrise to sunset 1931–1950 0130, 0730, 1330, 1930 1951–1954.
Parkersburg, West Virginia	39°16′	81°34′	185 [7]	Situated close to the general course of Little Kanowha River to the SE of Parkersburg. Two hills are close to the station, one 246 m elevation 1 km, to SW, the other 227 m elevation 1 km to ENE.	8 am & 8 pm 1900–1930 8 am, noon & 8 pm 1931–1936 7.30 am, noon & 7.30 pm 1937–1941 Av. daily cloudiness from 1942–1950 Av. daily cloudiness, sunrise to sunset 1951–1954.
Cheyenne, Wyoming	41°09′	104°49′	1839 [6]	Situated at the SE corner of Wyoming, on a broad ridge between the North Platte and South Platte Rivers. The terrain is rolling prairie. Ground level rises rapidly to a ridge of approx. 2700 m in elevation, about 48 km West.	6 am & 6 pm 1900–1930 Av. monthly cloudiness 1931–1950 0500, 1100, 1700 & 2300 1951–1954.

Table I: (continued)

Station	Latitude (N)	Longitude (W)	Ht(m) & [no. of locations]	Local description	Observation times
Lander, Wyoming	42°49′	108°44′	1669 [3]	Situated in Central Wyoming in the Valley of the Popo Agie River which lies at the foot and to the E. of the Wind River range. The airport station is 2.4 km SSE and approx. 60 m above the town. Terrain varies from rolling to broken; to the West and South West the foothills of the Wind River Range begin approx. 5 km from the station.	8 am & 8 pm 1900–1910 6 am & 6 pm 1911–1930 Av. daily cloudiness, sunrise to sunset, 1931–1950 0530, 1130, 1730, 2330 1951–1954.

the period 1900–1930. These two observations tend to be made at the same local time in the morning and the afternoon, which is often 4.30, 5.00 or 8.00 but can be other times. Sometimes between the years 1931 to 1939 or 1944 a third observation at noon is included. From the end of this sequence until 1948, only one monthly averaged cloud amount is reported for many stations which is stated to be a 'daylight average'. From the early 1950s to date, observations are made 4, 6 or more times during the 24–hr period and these individual averages are usually reported although occasionally they are returned only as a monthly mean.

Henderson-Sellers (1986) chose to use all the available observations to produce monthly average cloud amount for the two periods considered. The same technique was used here for the U.S.A. The one simplifying factor is that all the cloud amount reports contained in the Climatological Record Book are in tenths of sky cover, so no conversions were necessary in this work. The change in observing practice noted above unfortunately coincides with the categorization of years into the cold and warm periods examined here. It was thought possible that the unavoidable inclusion of additional observations into the second (warm) period data could affect the resulting cloud differences. Fortunately, for some stations the observations are reported separately rather than being averaged together. It was therefore possible to find 8 stations (10% of the total population) for which a test could be made of the impact of adding a midday observation to an average otherwise composed of a morning and evening observation only. The data are such that this investigation could be undertaken for 11 yr (1931–1941). A 90% signifance level was selected in order to decrease the Type II error (i.e. the chance of incorrectly accepting the null hypothesis when it is, in fact, false). Even at this level the null hypothesis could not be rejected, proving that in this data set there is no statistically significant difference between cloud averages including and excluding the noon observation.

Any use of surface-based observations of cloud amount necessitates assumptions about the accuracy of the observations. It is well established that cloud observations even by trained meteorologists will differ from individual to individual (e.g. Merritt, 1966). However there is less discrepancy between reports of total cloud amount than between assessment of cloud type and height (cf. discussion of example cloud scenes in Section 6). Also there is unlikely to be a systematic bias in the reports used here so that monthly means and hence the seasonal and annual averages analyzed should be fairly representative. Additionally each station can only be assumed to be representative of its immediate location. Malberg (1973) estimates that surface-based observations are typical of a circular area of radius ~50 km centred at the observing site. Thus an optimal spacing of observing sites (in ideal conditions) would be on a grid of dimension ~100 km. Unfortunately the other prerequisites precluded such an optimization in station choice here. Despite these problems the 77 stations selected from the data archive offer fairly good spatial coverage (Figure 3) and adequate temporal coverage (Table I). Although ~40% of the stations had small gaps in the 55 yr data run, there were very few stations for which these gaps were long. Typically 1 or 2 yr were missing, although for 3 stations (Tampa, Florida; Roswell, New Mexico and Reno, Nevada) there were gaps in both the warm and the cold periods. These stations were noted and were con-

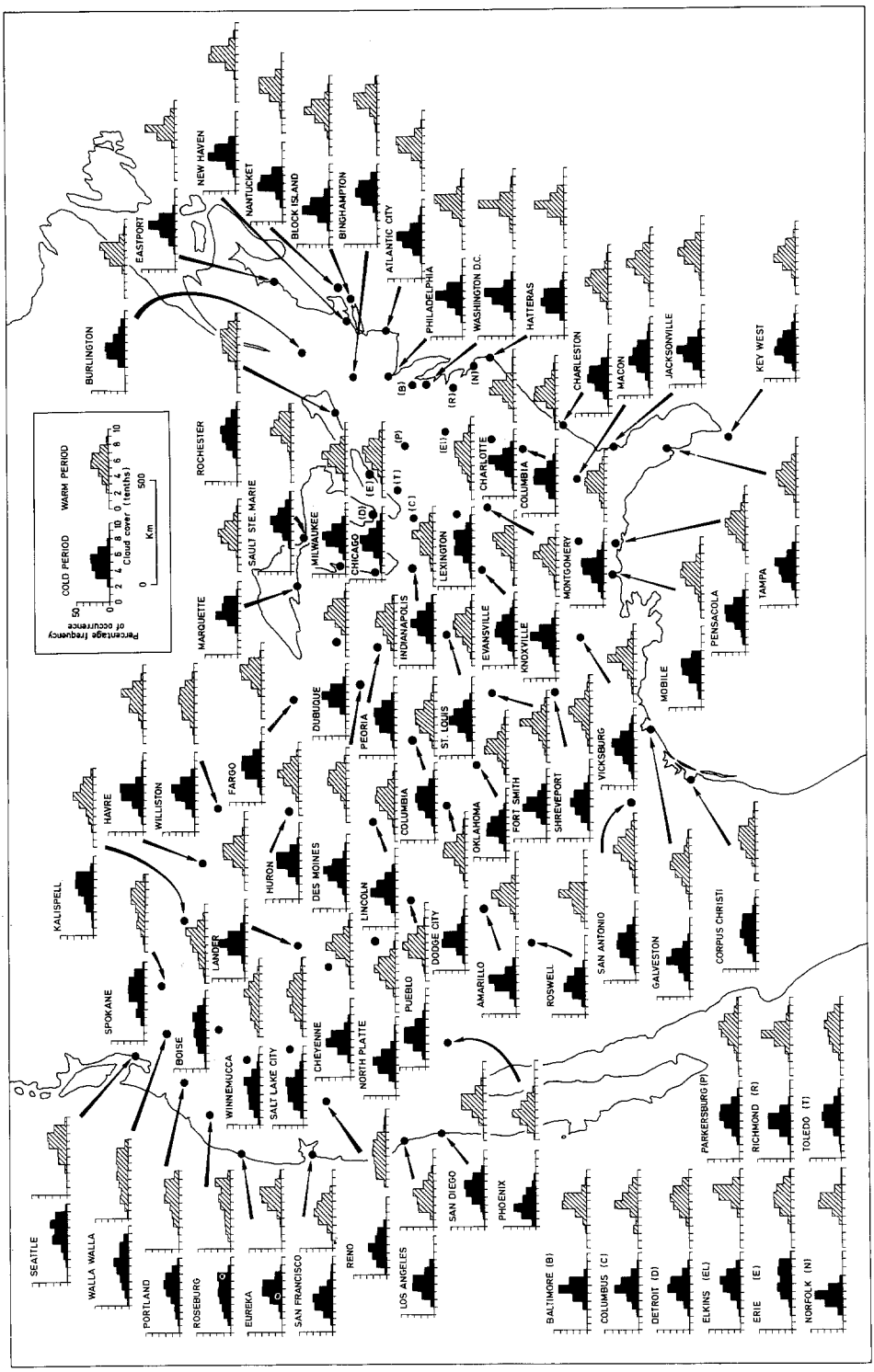

Fig. 3. Location of the 77 stations used in this study. The cloud characteristics are illustrated by a pair of histograms of percentage frequency of occurrence of mean monthly cloud amount for the cold and warm periods. Data for 68 stations are given *in situ* with the additional 9 stations being located by lettered points on the map.

sidered carefully when the cloud analyses were undertaken.

The characteristics of the cloudiness data for the cold and warm periods are illustrated in Figures 3 and 5. Histograms of percentage frequency of occurrence of cloud amount in tenths are shown for both periods in Figure 3. This type of representation of cloud data has been used to characterinze cloudiness regions (e.g. Barrett and Grant, 1979). The histograms show a somewhat surprising homogeneity with most of the stations having roughly normally distributed (bell-shaped) curves. Only two areas stand out: (1) stations in the northwest in and around Washington State show a wider spread of cloud amounts and (2) a few stations near Washington DC show much more 'peaked' frequency curves than is general. The tendency for the cloud amounts to be normally distributed is very much greater in the U.S.A. data than was the case for Europe (Figure 4) where there was a continental-scale trend from cloudy conditions in the northwest to generally clear skies in the southeast. In the U.S.A. map (Figure 3) there is a shift in the predominant cloud amount frequency (compare, for example, New Haven, Connecticut with Phoenix, Arizona) but often the shift between cold and warm periods is at least as marked (e.g. Burlington, Vermont and Elkings, West Virginia).

The trend from relatively cloudy conditions in the north to clearer skies in the south and central southwest is also apparent in the contour plots of seasonal and annual cloud amount for the two periods (Figures 5(i) and 5(ii)). However a more noticeable feature of the cloud amount contours shown in Figures 5(i) and 5(ii) is the increase in total cloud amount in all seasons and in the annual case between cold (Figure 5(i)) and the warm (Figure 5 (ii)) periods. The areas having less than 4 tenths cloud are greatly reduced in the warmer period. In the annual case the whole of central and southern U.S.A. changes from having less than 5 tenths cloud to having greater than 5 tenths. This increase in total cloud amount can also be seen in the annual cycle of cloud for the two periods shown for selected stations in Figure 5(iii). Most stations show increased mean monthly cloud amount in the warm period for most if not all months of the year and in certain locations, such as Norfolk, Virginia, this increase is considerable. Figure 5 (iii) also illustrates the variation in cloud amount over the United States; for example, cloud amounts reported in Seattle, Washington are often double those in Phoenix, Arizona. There are also many different seasonal cycles exhibited with Eastport, Maine and Norfolk, Virginia showing little seasonality, whilst cloudiness reaches a maximum in early summer in San Diego, California and a minimum in August in Salt Lake City, Utah.

The temporal and spatial consistency of the increase in cloud amount when moving from the cold to the warm period, which are shown in Figures 1, 2, and 5, are in direct contrast to the results which were described for Europe by Henderson-Sellers (1986) where there was much less coherence. The trends and differences in cloud amount for the warm and cold periods are analyzed in the following two sections.

4. Changing Cloud in a Warming World

Before examining the mean difference in cloud amount between the cold and warm periods (1901–1920 and 1934–1953) for the annual case and for the 4 seasons: March/

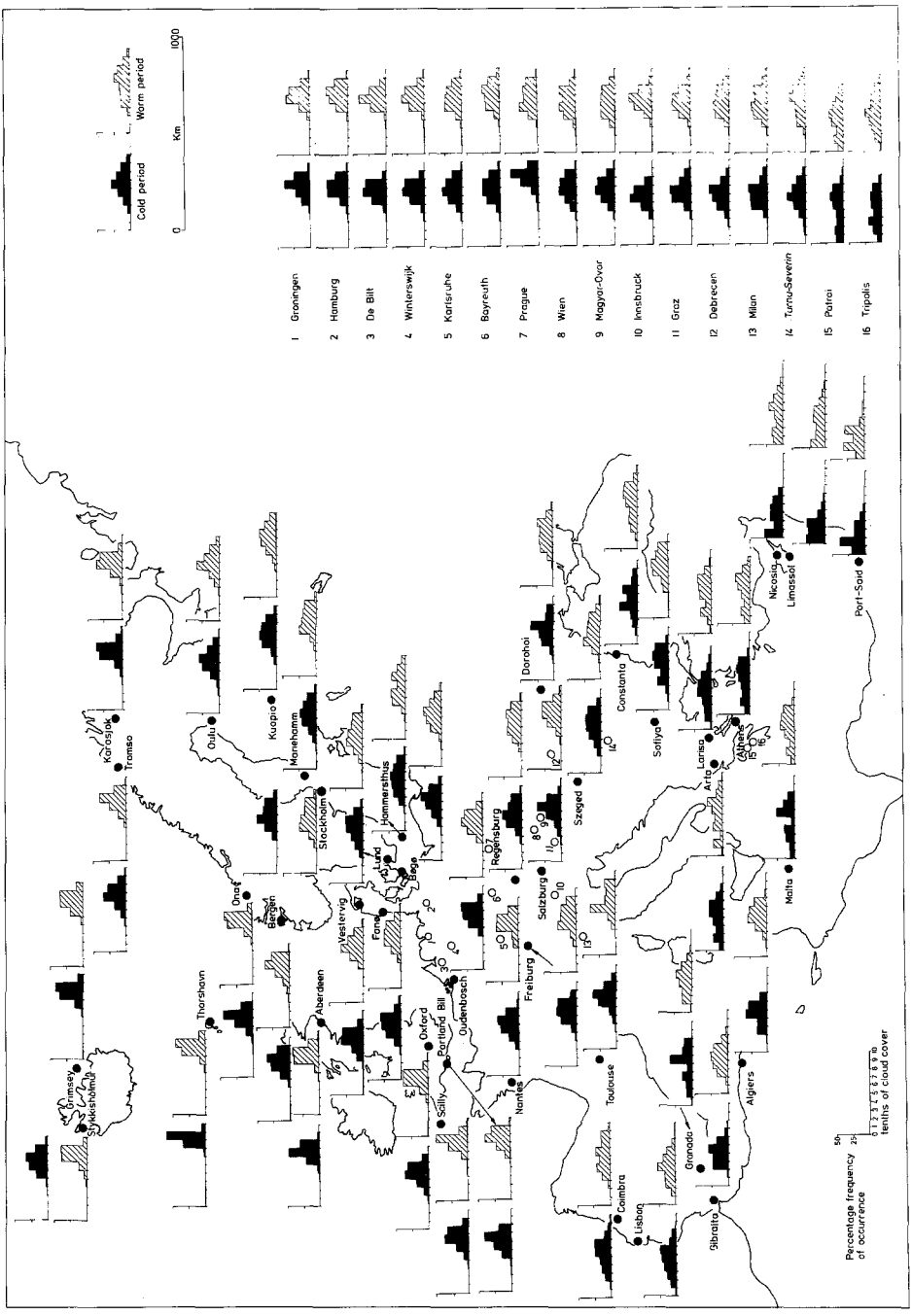

Fig. 4. Location and cloud frequency histograms for the cold and warm periods of the 58 European stations from Henderson-Sellers (1986).

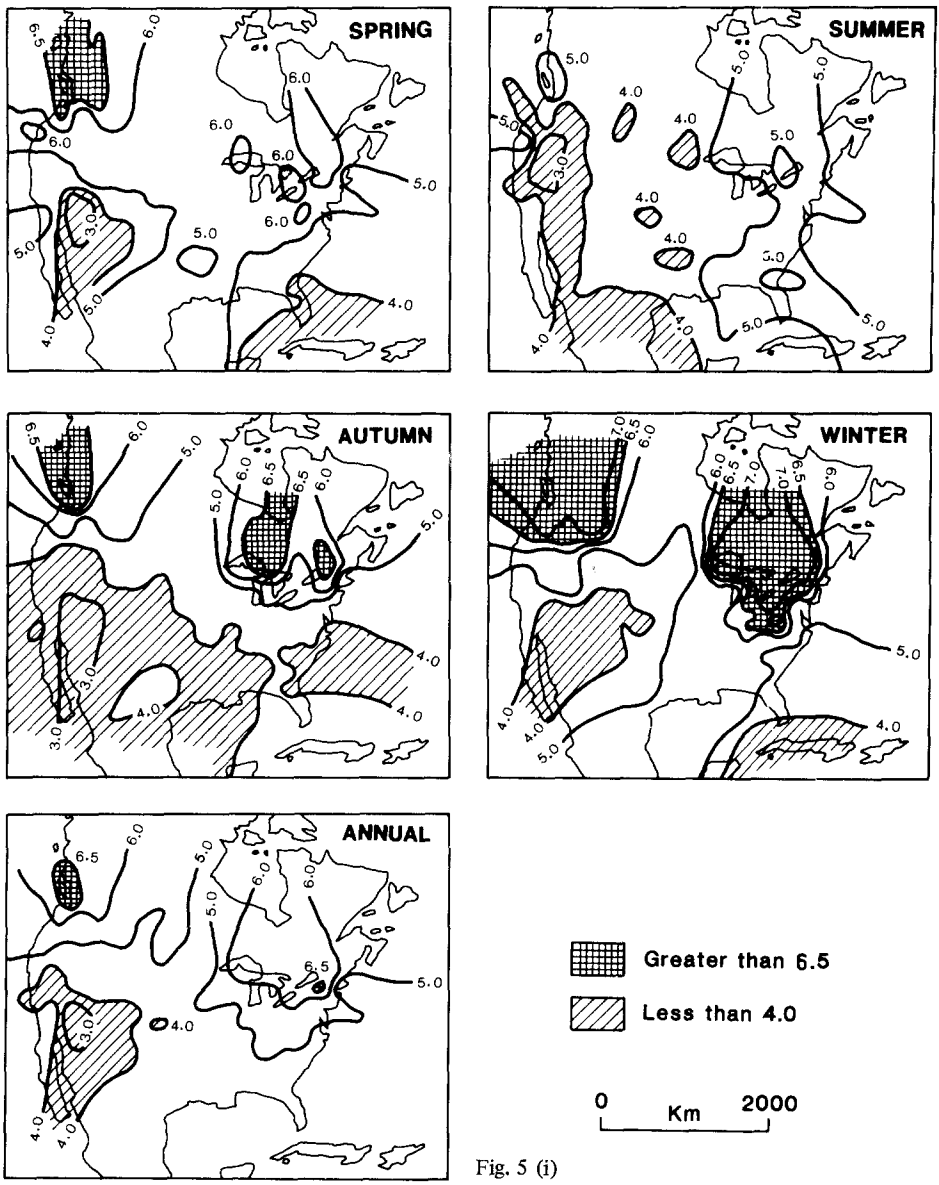

Fig. 5 (i)

Fig. 5 (i). Mean cloud amount in tenths for the cold period for the annual and four seasonal values. (ii) As for (i) for the warm period. (iii) Scattergraphs for selected stations: Seattle, San Francisco, Phoenix, San Diego, Sault Ste. Marie, Salt Lake City, Lincoln, Corpus Christi, Eastport, Norfolk, Columbia and Jacksonville. Mean and extreme values of monthly cloud amount for both the cold and warm periods are plotted.

April/May, June/July/August, September/October/November and December/January/February, it is necessary to establish whether there is any change in the variability between the two periods. The variability in cloud amount within each period about a medium term filtered trend has been computed so that any changes in variability would

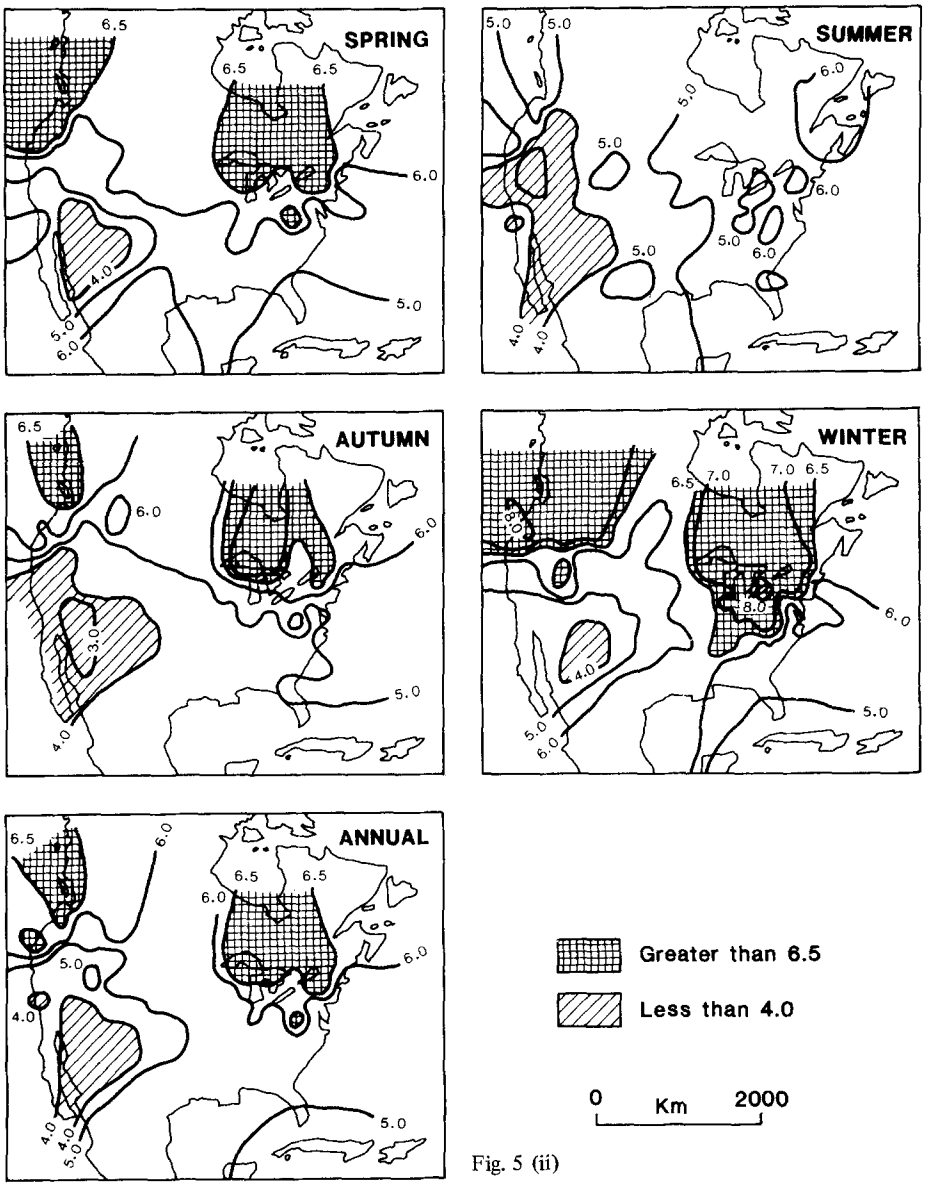

Fig. 5 (ii)

be decoupled from possible changes in mean values. In order to remove long time period (e.g. decadal) trends, a 1:2:1 binomial filter was applied to each of the 20 yr periods and the variances of the residuals from the filtered values analyzed. This is the same methodology as employed by Lough *et al.* (1983) and Henderson Sellers (1986). In order to retain a 20 yr filtered data set it was necessary to derive four more years' data: one at the beginning and end of each period analyzed.

The F test was applied to establish, at a 1% significance level, which stations exhibited a significant change in cloud variability between the cold and warm periods. The signifi-

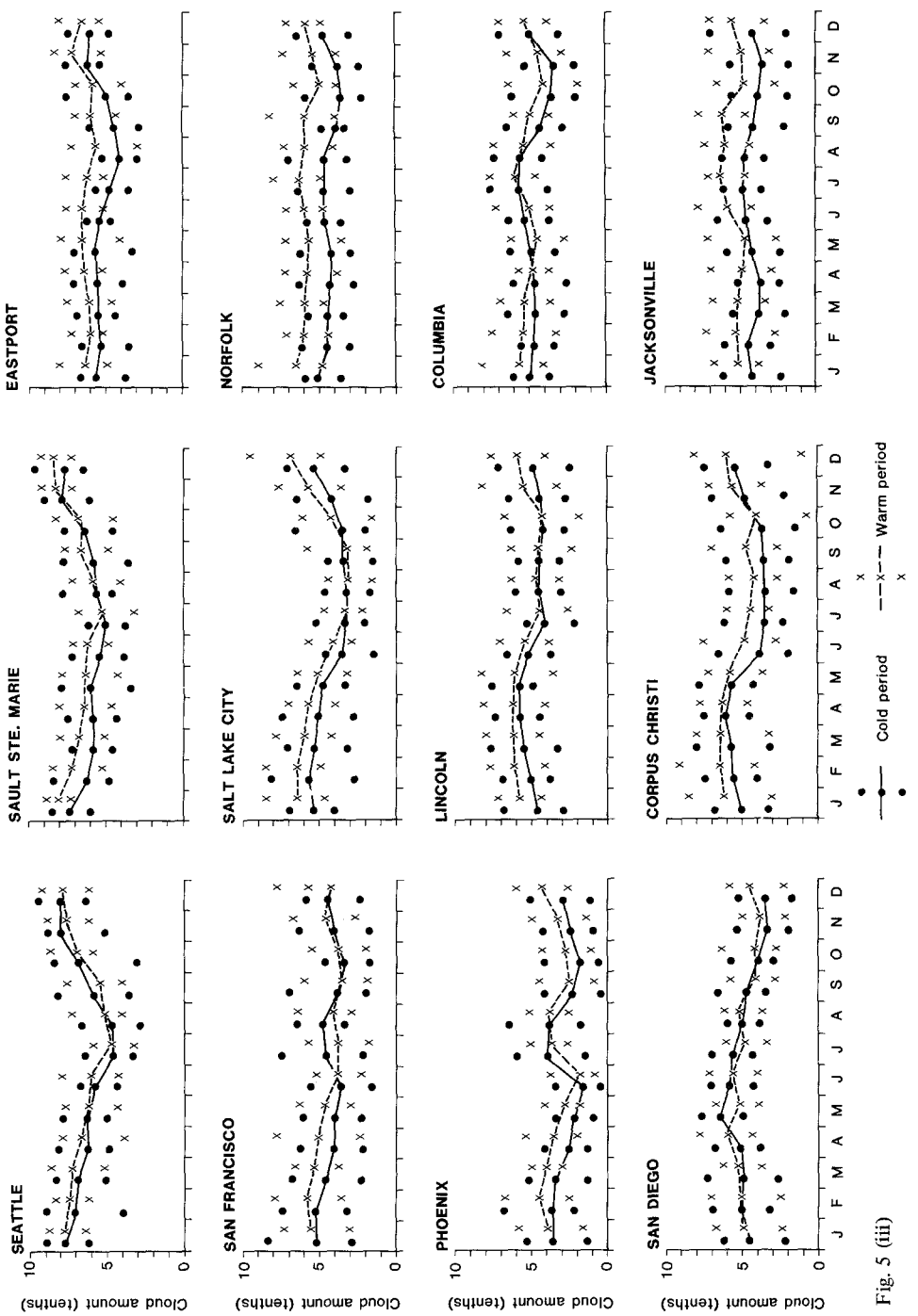
SEATTLE
SAULT STE. MARIE
EASTPORT
SAN FRANCISCO
SALT LAKE CITY
NORFOLK
PHOENIX
LINCOLN
COLUMBIA
SAN DIEGO
CORPUS CHRISTI
JACKSONVILLE
Cloud amount (tenths)
10
5
0
J F M A M J J A S O N D
Cold period
Warm period

Fig. 5 (iii)

cance level for this test was set at 1% in order that a Student's t test applied at the 5% level would be valid on the mean differences as described below (e.g. Figure 6).

Very few stations showed a significant change in cloud variability in the 'warming world'. No station exhibited statistically significant change in variability in more than 2 of the 5 time periods (4 seasons and annual) considered and only 7 of the 77 stations possessed this level of variability change. The season for which the greatest difference in variability was discovered was the spring (March/April/May) for which 16 stations failed to statisfy the criterion set for the F test. For the annual case 6 stations failed the F test at the 1% level and for summer, autumn and winter there were 4, 9 and 2 failures respectively. All stations for which the F test failed at the 1% level were excluded from the maps shown in Figure 6. Overall there is little evidence of a change in variability in cloudiness for most of the continental U.S.A. area analyzed in the warming world model. On the basis of this result the mean differences in cloud amount between the cold and warm periods have been analyzed as a function of the standard deviation of cloudiness over the complete 40 yr (i.e. 1901–1920 plus 1934–1953) period.

The mean difference (cold minus warm) in cloud amount for the annual and four seasonal cases is shown in Figure 6. The mean difference at each station has been divided by the normalized 40 yr standard deviation at that station. In the case where some data were missing the means and standard deviation have been appropriately modified. The resulting contours are of the Student's t statistic and are shown at the 5% and 0.1% levels for both increasing and decreasing cloudiness. Also shown is the -5 contour value for the Student t statistic.

The five maps show a very considerable degree of consistency. The whole of the eastern seaboard and the continental interior exhibits a large increase in cloud amount in the 'warming world'. Small areas on the western seaboard and in parts of the southwestern interior show less consistency and, in the summer season, there is a small area in the southwest which shows a statistically significant decrease in cloud amount. However, this is almost an unique occurrence in Figure 6 with the vast majority of the rest of the continental United States showing statistically significant increases in cloud in all seasons and in the annual case. These results underline the generally monotonic increase in cloudiness shown in Figures 1 and 2.

The results shown in Figure 6 are in considerable contrast to those reported by Henderson-Sellers (1986) for Europe. In the case of the application of the same warming world analogue model to Europe, a much more 'spotty' result was found (Figure 7). However, the maritime area of Europe did show an increase in cloud amount of a degree similar to that seen in Figure 6 for the U.S.A.. Figure 8 illustrates the general tendency for increased cloud in the annual case (Figure 8(a)) and even in the winter season (Figure 8(b)). There seems to be an important correlation between pressure patterns and cloudiness variation in these two studies. In the European case, there was an increase in sea-level pressure over the centre of the European area studied which was associated with smaller (or zero) temperature increases and with decreased cloud amounts; for example the winter cases seen in Figure 8(b), (c) and (d). For the U.S.A., sea-level pressure is lower by $\sim$1 hPa, temperature is higher, often by >1 °C, and cloudiness increases considerably.

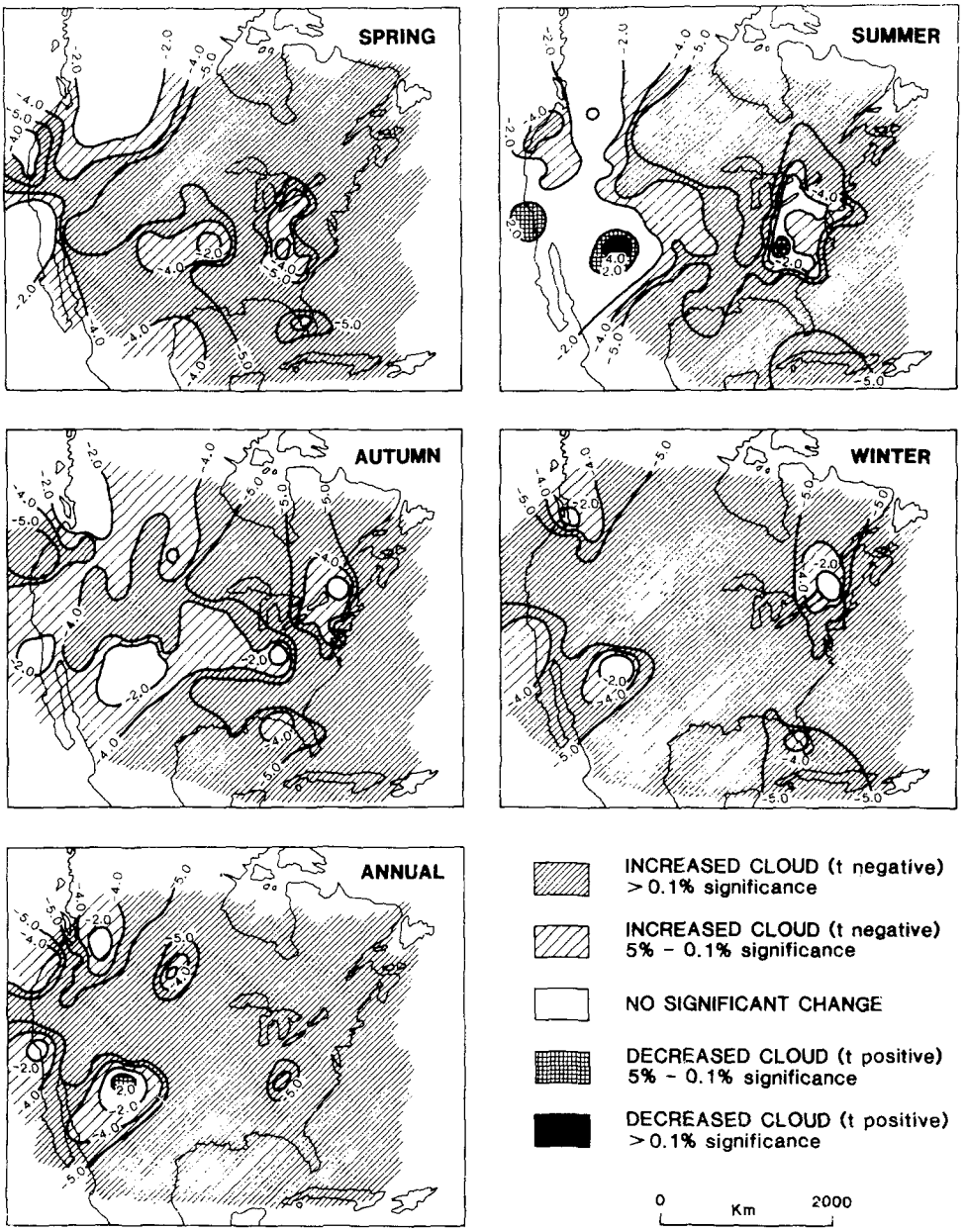

Fig. 6. Variation of the Student's t statistic for the U.S.A. generated from the mean differences (cold minus warm period) for the annual and seasonal cases. A negative difference (cold – warm) suggests an increase in cloudiness in a warmer world. The values at each station have been normalized by the station standard deviation for the 40 yr divided by $\sqrt{n}$ where n is the number of years for which valid data were available. While the zones of 5% significance have been shown to be statistically valid an additional test of the variances at a higher significance level would be required to demonstrate the validity of the 0.1% contours shown.

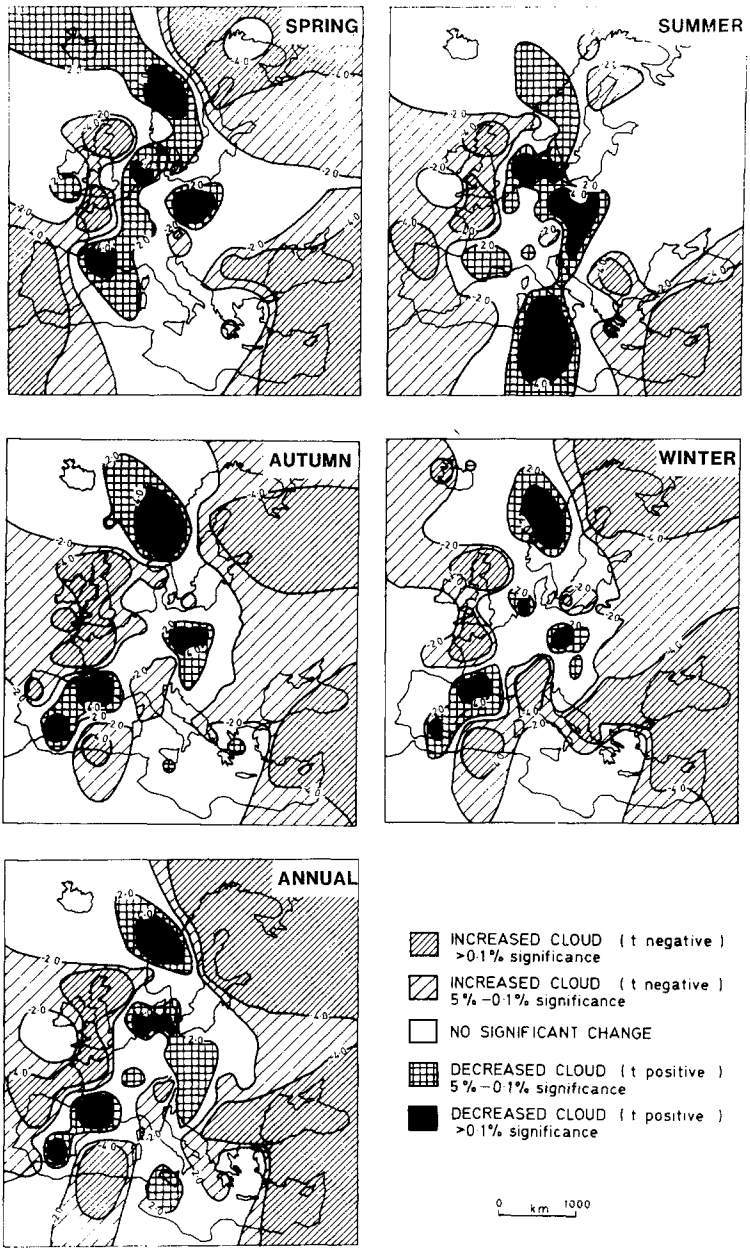

Fig. 7. Variation of the Student's t statistic for Europe generated from the mean differences (cold minus warm period) for the annual and seasonal cases. A negative difference (cold – warm) suggests an increase in cloudiness in a warmer world. The values at each station have been normalized by the station standard deviation for the 40 yr divided by $\sqrt{n}$ where n is the number of years for which valid data were available. While the zones of 5% significance have been shown to be statistically valid an additional test of the variances at a higher significance level would be required to demonstrate the validity of the 0.1% contours shown (after Henderson-Sellers, 1986).

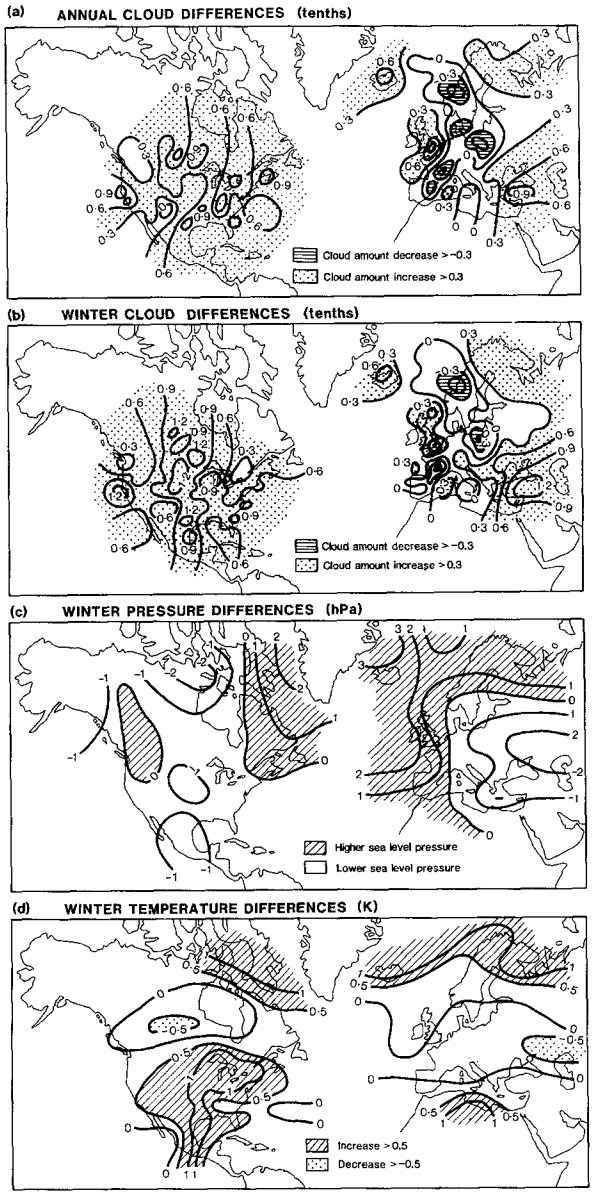

Fig. 8 (a). Differences in tenths of sky cover between annual mean cloud (warm period – cold period) derived from the data described here and in Henderson-Sellers (1986). (b) Differences in tenths of sky cover between winter (December/January/February) mean cloud (warm period – cold period) derived from the data described here and in Henderson-Sellers (1986). (c) Sea-level pressure differences for winter (December/January/February) warm period minus cold period. (d) Temperature differences for winter (December/January/February) warm period minus cold period. (c) and (d) have been redrawn from Palutikof *et al.* (1984) and Lough *et al.* (1983).

In the European case, pressures have risen over the central part of the area considered due to increased blocking by anticyclones. The wintertime temperatures have decreased, by up to 0.5 °C, perhaps causing the decrease in cloud over the central part of the area. On the other hand, there remains increased cloud cover over the maritime and central continental areas of Europe. In the case of the U.S.A., the generally lowered pressures would tend to increase the frequency of southerly air flows which might be the cause of both the increased temperatures in the eastern and central region and the increased cloudiness. It is possible that the east/west contrast in degree of cloud increase seen in Figure 6 (especially in the summer season) may be associated with the influence of the Rocky Mountains. They would tend to block the southerly air flow producing cooler and, perhaps, slightly less cloudy conditions in the western part of the continent. Despite this, the whole of the U.S.A. exhibits increased cloud amounts, as well as increased temperatures, in common with approximately half the European area studied earlier.

5. Transient v. Equilibrium Climate Changes

The basis of this historical analogue investigation of climate change is transient change in climate characteristics. To date all published GCM experiments have considered a change in the equilibrium state of the climate. It is not at all clear that transient changes are useful analogues of the differences between equilibrium states. Indeed the data base described here can be used to demonstrate that transient variations occurring over different time-scales give rise to very different models of climate change.

Figure 9 compares the cloud changes between two contrasting cold/warm periods. Figure 9(a) shows the mean cloud differences (December/January/February (winter) minus June/July/August (summer)) for the cold period (1901–1920) and Figure 9(b) the same difference for the warm (1934–1953) period. In each case the mean cloud difference has been divided by the normalized pooled standard deviation of the cloudiness for the two seasons for the 20 yr period. The contours are drawn in increments of normalized pooled station standard deviation. The contrast between these maps and the annual case from Figure 6 which is reproduced as Figure 9(c) is apparent. Seasonally cloud amount decreases in moving from cold (winter) to warm (summer) conditions whereas temporally the warming world analogue model shows that cloud amount increases over the U.S.A. (cf. Figures 1 and 2). This result underlines the earlier, and more tentative, conclusion of Henderson-Sellers (1986): that it is certainly insufficient and probably incorrect to infer that a seasonally verified cloud prediction scheme in a GCM will, *de facto*, be appropriate in a warming world situation (cf. Warren and Schneider, 1979). More importantly Figure 9 demonstrates that, for the case of total cloud amount, seasonal changes are not a useful model for longer term (e.g. decadal) transient changes. This result could have important consequences for numerical model validation. Some of these are explored in the next section.

The contrast between the transient analogue model cloud changes found here and equilibrium GCM simulations is considerable. Hansen *et al.* (1984) show a map of predic-

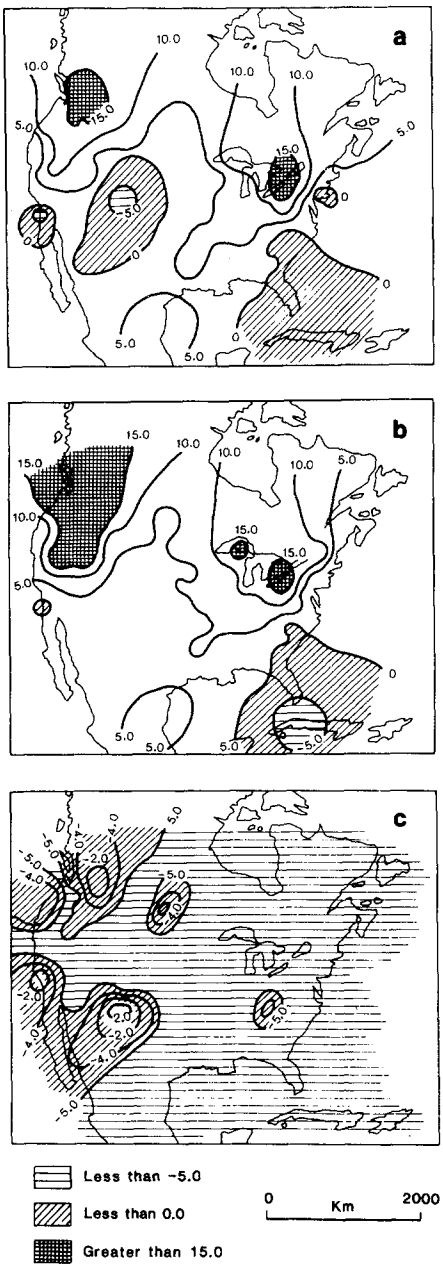

Fig. 9 (a). Normalized differences between the winter (DJF) and summer (JJA) seasons (i.e. DJF–JJA) for the cold period. The normalizing factor is the pooled standard deviation at each station divided by $\sqrt{[n_1 n_2/(n_1+n_2)]}$ where n_1 and n_2 are the number of valid data items for winter and summer within each 20 yr period. (b) As for (a) but for the warm period. [Contour values in (a) and (b) are of mean difference divided by the normalized standard deviation and are therefore directly comparable with the contour values in Figure 6] (c) Annual case from Figure 6. Shading redrawn to be the same as (a) and (b).

ted change in total cloud amount derived from differencing averages from two 5 year simulations. In this doubled CO_2 experiment, in which the global mean temperatures rose by around 4 °C, they show cloud amount changes over Europe and the continental USA of between 0 and −0.3 tenths. This prediction of decreased cloud amount is in agreement with cloud changes obtained using other GCMs. Washington and Meehl (1984), using the NCAR GCM, and Wetherald and Manabe (1980), using the GFDL model, also predicted cloud amount decreases in increased CO_2 experiments. Wetherald and Manabe (1986) have conducted a detailed investigation of cloud cover changes occurring in response to thermal forcing in numerical climate models. They conclude that increased CO_2 experiments show a general reduction in tropospheric cloud cover. The results they obtained from five separate numerical climate model experiments are in qualitative agreement with the results from the GISS and NCAR GCMs, suggesting that cloudiness is reduced in the tropical and mid-latitude rainbelt regions and increased in the stable layer near the Earth's surface from middle to high latitudes as a result of increased thermal forcing.

The historical analogue model does not reveal the direction of cloud-climate feedback because there is no information about cloud type and because no cause-and-effect mechanism between temperature and cloud changes has been shown. The radiative impact of the cloud changes predicted by the two contrasting experiment types is extremely difficult to establish. In both the transient (analogue) and the equilibrium (GCM) experiments the cloud amount change is $\lesssim 1$ tenth in total cloud cover. Wilson and Mitchell (1986) find, in a study of North Africa, that increasing the low cloud amount by ~1 tenth reduces the solar flux at the surface by ~85 W m^{-2}. Perhaps more importantly, they find that the diurnal cycle is degraded in a GCM in which the cloud amount is incorrectly specified or maintained. Despite these considerable caveats the differences between these numerical model results and those of the historical cloud analogue model described here are rather tantalizing. Considering the simplest possible case of a constant effective cloud top height, the equilibrium numerical model results predicting decreased cloud amount would tend to increase further the predicted surface temperature increases. On the other hand, the real world transient experiment seems to suggest increased cloud amount which, again assuming no change in cloud type or height, might lead to a negative feedback on surface temperatures.

6. Discussion: Employing Surface-observed Cloudiness Data in Climate Sensivity Studies

Investigation of the sensitivity of the climate system should involve comparisons of observed and modelled results on all accessible time and space scales. There is, unfortunately, a hesitancy among many climate modellers about utilising surface retrieved cloud information. This reluctance is understandable in one sense, since surface observations of cloud suffer from many limitations. The data are predominantly continental and are biased towards low cloud amount. Numerical models, on the other hand, predict multi-layer clouds using a variety of prediction schemes. The extent of the differences

amongst currently used cloud prediction schemes was recently highlighted by Schlesinger and Mitchell (1985) in the context of a comparison of the performance of three GCMs in a numerical simulation of the climatic impact of doubling atmospheric CO_2. They compared the numerical and physical parameterization schemes used in the NCAR, GFDL and GISS GCMs. Table II summarises the model cloud prediction schemes.

All three models form clouds by both largescale condensation and convection. Large-scale clouds are predicted when the relative humidity exceeds 80%, 99% and 100% in the NCAR, GFDL and GISS models respectively, with the amount of coverage being set at 95%, 100% and 100% respectively; although the GISS model assigns cloud cover in the grid box for only a certain percentage of the time (the percentage being based on a scheme which compares the fraction of the grid box that is saturated to a random number generated in the interval 0–1). Convective cloud is predicted when there is moist convection although the GISS model actually generates convective cloud only when another test based upon a random number generator is satisfied. Convective cloud is 100% in the GFDL and GISS models and 30/N (%) per layer in the NCAR model, where N is the number of layers undergoing convection.

The optical properties of the clouds depend on the cloud height in all three models; in the NCAR model optical properties are also a function of the solar zenith angle and in the GISS model the optical depth is a function of temperature, pressure and pressure thickness (see Table II). The treatment of terrestrial and solar radiation is otherwise very similar in all three models, although the value of the solar constant differs, being 1367, 1370, and 1467 W m^{-2} in the GISS, NCAR and GFDL models respectively. Only the GISS model includes the diurnal as well as the seasonal cycle. The resulting layer cloud amount is global but may be biased by other model characteristics such as the specification of sea surface temperature or of ocean mixed layer depth, sea ice extent, soil moisture variability etc. Also 'total' cloud amount is generally computed from the layer cloud predictions using the assumption of random overlap. Despite these inherent differences most modelling groups are quite prepared to display global maps of predicted cloud and compare these with surface observations of cloudiness. For example, Washington and Meehl (1984) compare the NCAR GCM cloud predictions with the cloud data of London (1957), Hansen *et al.* (1983) compare the GISS GCM cloud predictions with surface observations collected together by Berry *et al.* (1973), Potter and Gates (1984) use the predominantly surface observed cloud archive of Berlyand and Strokina (1980) and Wilson and Mitchell (1986) choose observational data from Meleshko and Wetherald (1981) which is, in fact, a combination of an earlier version, 1974, of Beryland and Strokina and the southern hemisphere data of Van Loon *et al.* (1972).

The recognition by climate modellers of the verity of surface observed cloudiness information does not require an act of faith since it is demonstrably easier to retrieve sophisticated and fairly accurate cloud information than to measure accurately most other meteorological parameters. Figure 10 shows two cloud images. From these any untrained observer can make a reasonable cloud amount assessment and training improves recognition capabilities. For example, the halo around the Sun in Figure 10(b) indicates the existence of cirrus cloud. The human eye/brain combination has been able to deter-

TABLE II: Comparison of the cloud prediction schemes used in three GCMs (after Schlesinger and Mitchell, 1985).

GISS

Clouds are allowed to form in each layer below 100 hPa due to large-scale condensation and cumulus convection. A large-scale cloud can occur when $RH > 100\%$; cloud cover $C = 0$ if $f_s < N_r$ and $C = 1$ if $f_s > N_r$, where f_s is the saturated fraction of a gridbox obtained under the assumptions that the absolute humidity is uniform throughout the gridbox and the temperature has a prescribed Gaussian subgrid-scale form, and N_r is a generated random between 0 and 1. A convective cloud can occur when there is cumulus convection; cloud cover $C = 0$ if $\gamma M < N_r$ and $C = 1$ if $\gamma M > N_r$, where M is the mass of saturated air rising through the base of a layer and $\gamma = 2.5$ m^3 s kg^{-1}. Optical depth for large-scale clouds $\tau = 1/3$ for $T < 258$ K and $\tau = 0.0133\,(p - 100)$ for $T > 258$ K, where T is the layer temperature and p is the level pressure in hPa. For convective clouds $\tau = 0.08\,\Delta p$ where Δp is the cloud pressure thickness in hPa. Cloud absorptivity and emissivity are derived from phase function and single-scattering albedo based on Mie computations with radii of 10 μm and 25 μm for water and ice clouds, respectively.

NCAR

Clouds are allowed to form in each layer above the lowest layer and below 250 hPa for $|\phi| < 45°$ and below 400 hPa for $|\phi| > 45°$ latitude due to large-scale condensation and cumulus convection. A large-scale cloud occurs when $RH > 80\%$ with a cloud cover C = 0.95. Convective cloud occurs when $\partial\theta_e/\partial z < 0$ and $RH > 80\%$ with $C = 0.30/N$ in each of the N layers undergoing moist convective adjustment. Clouds in different layers are assumed to be randomly overlapped. Cloud albedo $\alpha = \beta\mu/(\beta + \cos\zeta)$ where ζ is the zenith angle, $\mu = \min(1, \sqrt{[LWC/100]})$ with LWC (kg m^{-2}) the column condensate during one hour of model time, $\beta = 0.6$, 0.3, 0.15 for low ($0.811 \leqslant \sigma \leqslant 0.991$), middle ($0.5 \leqslant \sigma \leqslant 0.811$) and high ($\sigma < 0.5$ and $p > 250$ hPa for $|\phi| < 45°$ and $p > 400$ hPa for $|\phi| > 45°$ latitude), respectively. For clouds occuring simultaneously in two or more layers, the albedo is taken equal to the maximum over all the layers. Cloud absorption only by water vapour and ozone. Emissivity $\epsilon = 1$ for high cloud and $\epsilon = \mu$ for middle and low clouds.

GFDL

Clouds are allowed to form in each layer. Large-scale cloud occurs when $RH > 99\%$ with a cloud cover $C = 1.0$. Convective cloud occurs when $\partial\theta_e/\partial z < 0$ and $RH > 100\%$ with $C = 1.0$. For thin clouds (existing in one layer only), the albedo and absorptivity for $\lambda < 0.7$ μm ($\lambda > 0.7$ μm) are 0.21 (0.19) and 0.0 (0.04) for high cloud (>10.5 km), and 0.45 (0.35) and 0.0 (0.2) for middle cloud (~4.0 to 10.5 km), 0.65 (0.55) and 0.0 (0.30) for low cloud (0.0 to 4.0 km). For thick cloud (existing in two or more contiguous layers), the albedo and absorptivity are 0.57 (0.47) and 0.0 (0.3). The emissivity is 0.6 for high cloud and unity for middle and low cloud.

mine cloud structure and optical properties for very much longer than radiance-based retrieval algorithms. The level of agreement between trained observers is also better than the current level of agreement amongst a range of satellite-based cloud retrieval algorithms (cf. Rossow *et al.*, 1985). Climate modellers are tempted to reject surface-observed cloud information either because of the spatially restricted nature of the data or because satellite-retrieved cloudiness seems more amenable to comparison with model-predicted cloud amount. Indeed the goal of the International Satellite Cloud Climatology Project is to produce radiatively 'effective cloud' for comparison with or insertion into numerical climate models. These radiatively correct 'clouds' can natuarally be expected to produce radiatively correct fluxes, but validation of numerical climate models must not depend solely on such intercomparisons.

An alternative and complementary strategy is to devise a method of computing 'sur-

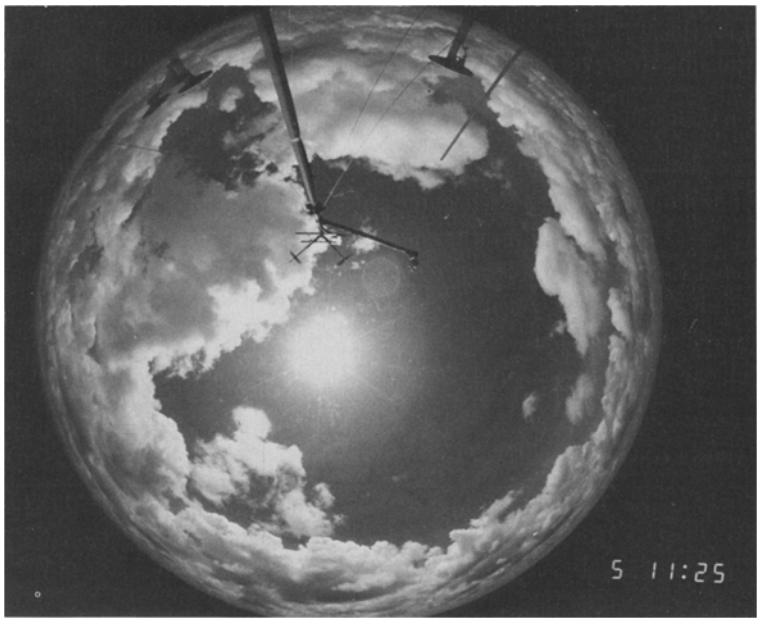

(a)

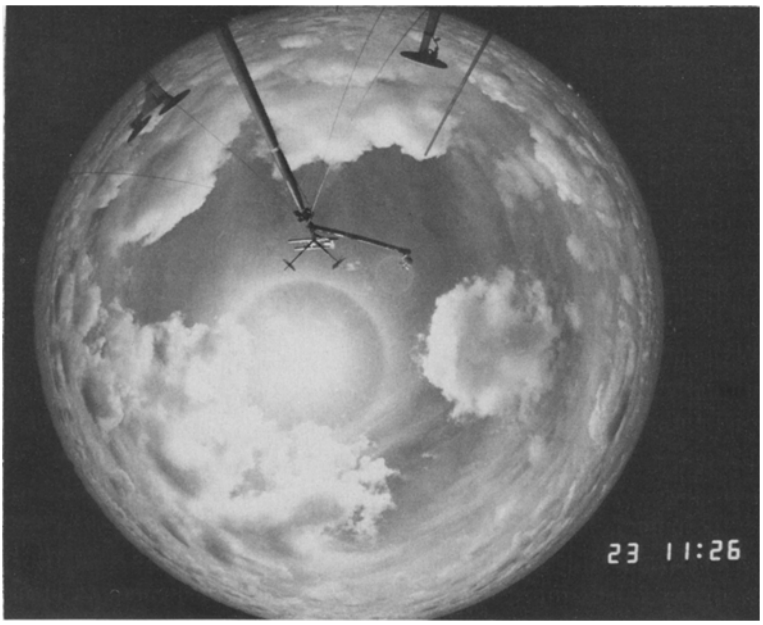

(b)

Fig. 10 (a). All-sky camera photo taken on 5 April, 1985 (11:25 LT) showing towering cumulus cloud. (b) All-sky camera photo taken on 23 April, 1985 (11:26 LT) showing cumulus cloud underlying a cirrus overcast.

face-observed' clouds from numerical models. (This is actually no more difficult than attempting to compute 'satellite-observed' clouds from multi-layer spatially homogeneous model predicted clouds). These cloud characteristics could be compared with current surface observations of clouds, including cloud type, amount, structure and possibly even basic optical properties. A preliminary example of the potential use of surface-observed cloudiness in the interpretation of radiative fluxes and climate model predictions was made by Ohring and Gruber (1983) when they introduced the concept of locationally specific climatologies determined from satellite data. There is every reason to believe that comparison of regional and seasonal cloudiness characteristics could aid in the improvement of cloud prediction schemes in numerical models. With the increasing recognition of the importance of adequate prediction of the land surface climate, it would also be worthwhile to try to compare the diurnal variation of predicted and observed cloudiness (cf. Wilson and Mitchell, 1986).

It does not seem too far-fetched to contemplate a surface-based equivalent of the International Satellite Cloud Climatology Project. In this study a number of regions would be identified as being of climatological interest and importance. (This identification would almost certainly be based on ISCCP data). At a number of sites within these regions surface observations of cloud amount, type and characteristics would be made together with measurement of radiative fluxes. These observations would be complementary to satellite-retrievals of radiation and cloud made at the top of the atmosphere. Numerical climate models should be able to reproduce upper and lower boundary conditions correctly.

It is, of course, essential that cloud type (i.e. radiation parameters and cloud height) be predicted successfully (Charlock and Ramanathan, 1985) as well as total cloudiness. Radiative properties depend on the liquid water path not cloud amount (e.g. Wang *et al.*, 1981; Charlock, 1982; Somerville and Remer, 1984). The observational data such as those described here offer little information about these other characteristics. However, the results presented here, although tentative, seem to suggest a trend of increasing total cloud amount associated with increasing temperatures during the first half of this century. Of course it is possible that the increase in cloud seen in the historical data is all high, thin cloud which tends to warm the surface not cool it (Ramanathan *et al.*, 1983). The historical cloud data collected so far do not permit analysis of anything other than total cloud amount. Even so, the climate modelling community should be encouraged to try to simulate these, and other, observational trends as well as concentrating upon compatability between satellite-retrieved radiances and cloudiness.

Acknowledgements

I am grateful to Ms Mary Benbow who collected the data from the archives. I also wish to thank the U.S. Air Force staff at Operating Location A, North Carolina who made work space available for her so that the very large number of volumes of meteorological records could be consulted. This research was sponsored in part by the Air Force Office of Scientific Research, Air Force Systems Command, USAF under grant number AFOSR–

86–0118. The U.S. Government is authorised to reproduce and distribute reprints for Governmental purposes notwithstanding any copyright thereon. Finally I am grateful to Bill Rossow, Peter Webster, Dick Wetherald and Bob Dickinson for critical reviews of an earlier version of this paper.

References

Barrett, E. C. and Grant, C. K.: 1979, 'Relations Between Frequency Distributions of Cloud Cover over the United Kingdom Based on Conventional Oberservations and Imagery from Landsat-2, *Weather* **34**, 416–423.

Berlyand, T. G. and Strokina, L. A.: 1974, 'Cloudiness Regime over the Globe', *Phys. Climatol.* MGO Trudy, **338**, 3–20.

Berlyand, T. G. and Strokina, L. A.: 1980, *Global Distribution of the Total Amount of Cloudiness*, Hydrometeor. Pub., Leningrad, USSR.

Berry, F., Bollay, E., and Beers, N. (eds.): 1973, *Handbook of Meteorology*, McGraw-Hill, 1068 pp.

Brewer, P. G.: 1978, 'Direct Observations of the Oceanic CO_2 Increase, *Geophys. Res. Lett.* **5**, 997–1000.

Cess, R. D., Briegleb, B. P., and Lian, M. S.: 1982, 'Low-Latitude Cloudiness and Climate Feedback: Comparative Estimates from Satellite Data', *J. Atmos. Sci.* **39**, 53–59.

Charlock, T. P.: 1982, 'Cloud Optical Feedback and Climate Stability in a Radiative-convective Model', *Tellus* **34**, 245–254.

Charlock, T. P. and Ramanathan, V. : 1985, 'The Albedo Field and Cloud Radiative Forcing Produced by a General Circulation Model with Internally Generated Cloud Optics', *J. Atmos. Sci.* **42**, 1408–1429.

Chen, C. T. and Millero, F. J.: 1979, 'Gradual Increase of Oceanic Carbon Dioxide', *Nature* **277**, 205–206.

Dickinson, R. E. and Cicerone, R. J.: 1986, 'Future Global Warming from Atmospheric Trace Gases', *Nature* **319**, 109–115.

Flohn, H. : 1977, 'Climate and Energy: A Scenario to a 21st Century Problem', *Climatic Change* **1**, 5–20.

Folland, C. K., Parker, D. E., and Kates, F. E.: 1984, 'Worldwide Marine and Temperature Fluctuations 1856–1981', *Nature* **310**, 670–673.

GARP/JOC: 1978, *JOC Study Conference on Parameterization of Extended Cloudiness and Radiation for Climate Models,* Oxford, England, GARP Climate Dynamics Sub-programme, WMO, Geneva.

Gates, W.L.: 1980, *A review of Modelled Surface Temperature Changes Due to Increased Atmospheric CO_2*, Climatic Research Institute Rep. No. 17, Oregon State University, Corvallis, 21 pp.

Hansen, J., Lacis, A., Rind, D., Russell, G., Stone, P., Fung, I., Ruedy, R., and Lerner, J.: 1984, 'Climate Sensitivity: Analysis of Feedback Mechanism', in J.E. Hansen and T. Takahashi (eds.), *Climate Processes and Climate Sensitivity*, American Geophysical Union, Washington, D.C., pp. 130–163.

Hansen, J., Russell, G., Lacis, A., Fung, I., Rind, D., and Stone, P., 1985, 'Climate Response Times: Dependence on Climate Sensitivity and Ocean Mixing', *Science* **229**, 857–859.

Henderson-Sellers, A.: 1986, 'Cloud Changes in a Warmer Europe', *Climatic Change* **8**, 25–52.

Hughes, N. A.: 1984, 'Global Cloud Climatologies: An Historical Review', *J. Clim. Appl. Meteor.* **23**, 724–751.

Jäger, J. and Kellogg W. W.: 1983, 'Anomalies in Temperature and Rainfall During Warm Arctic Seasons', *Climatic Change* **5**, 39–60.

Jones, P. D., Wigley, T. M. L., and Kelly, P. M.: 1982, 'Variations in Surface Air Temperature, Part 1: Northern Hemisphere, 1881–1980', *Mon. Weath. Rev.* **110**, 59–70.

Jones, P. D., Raper, S. C. B., Bradley, R. S., Diaz, H. F., Kelly, P. M., and Wigley, T. M. L.: 1986, 'Northern Hemisphere Surface Air Temperature Variations: 1851–1984', *J. Clim. Appl. Meteor.* **25**, 161–179.

Kellogg, W. W.: 1977, *Effects of Human Activities on Climate*, WMO Tech. Note 156, WMO No. 486, World Meteorological Organization, Geneva.

Kellogg, W. W. and Schware, R.: 1981, *Climatic Change and Society, Consequences of Increasing Atmospheric Carbon Dioxide,* Westview Press, 178 pp.

London, J.: 1957, *A Study of the Atmospheric Heat Balance,* AFCRC-TR-57–287, College of Engineering, New York University, N.Y.

Lough, J. M., Wigley, T. M. L., and Palutikof, J. P., 1983, 'Climate and Climate Impact Scenarios for Europe in a Warmer World', *J. Clim. Appl. Meteor.* **22**, 1673–1684.

Malberg, H.: 1973, 'Comparison of Mean Cloud Cover Obtained by Satellite Photographs and Ground Based Observations over Europe and the Atlantic', *Mon. Weath. Rev.* **101**, 893–897.

Manabe, S. and Wetherald, R. T.: 1975, 'The Effects of Doubling the CO_2 Concentration on the Climate of a General Circulation Model', *J. Atmos. Sci.* **32**, 3–15.

Meleshko, V. and Wetherald, R. T.: 1981, 'The Effect of a Geographical Cloud Distribution on Climate: A Numerical Experiment with an Atmospheric General Circulation Model', *J. Geophys. Res.* **86**, 11995–12014.

Merritt, E. S.: 1966, 'On the Reliability and Representativeness of Sky Cover Observations', *J. Appl. Meteor.* **5**, 369.

Mitchell, J. F. B.: 1983, 'The Seasonal Response of a General Circulation Model to Changes in CO_2 and Sea Temperatures', *Quart. J. Roy. Meteor. Soc.* **109**, 113–152.

National Academy of Science (NAS): 1982, *Carbon Dioxide and Climate: A Second Assessment,* National Academy Press, Washington, D.C., 72 pp.

Ohring, G. and Clapp, P. F.: 1980, 'The Effect of Changes in Cloud Amount on the Net Radiation at the Top of the Atmosphere', *J. Atmos. Sci.* **37**, 447–454.

Ohring, G. and Gruber, A.: 1983, 'Satellite Radiation Observations and Climate Theory', in B. Salzman (ed.), *Theory of Climate,* Advances in Geophysics, Volume 25, Academic Press, New York, pp. 237–304.

Palutikof, J. P., Wigley, T. M. L., and Lough, J. M.: 1984, *Seasonal Climate Scenarios for Europe and North America in a High-CO_2, Warmer World,* Carbon Dioxide Research Division of Dept. of Energy, Report No. TRO 12 (available from NTIS, Springfield VA 22161), 70 pp.

Pittock, A. B. and Salinger, J. M.: 1982, 'Towards Regional Scenarios for a CO_2-warmed Earth, *Climatic Change* **4**, 23–40.

Potter, G. L. and Gates, W. L.: 1984, 'A Preliminary Intercomparison of the Seasonal Response of Two Atmospheric Climate Models, *Mon. Wea. Rev.* **112**, 909–917.

Ramanathan, V., Pitcher, E. J., Malone, R. C. and Blackmon, M. L.: 1983, 'The Response of a Spectral General Circulation Model to Refinements in Radiative Processes', *J. Atmos. Sci.* **40**, 605–630.

Rossow, W. B., Moscher, F., Kinsella, E., Arking, A., Desbois, M., Harrison, E., Minnis, P., Ruprecht, E., Sèze, G., Simmer, C., and Smith, E.: 1985, 'ISCCP Cloud Algorithm Intercomparison', *J. Clim. Appl. Meteor.* **24**, 877–903.

Schiffer, R. A. and Rossow, W. B.: 1983, 'The International Satellite Cloud Climatology Project (ISCCP). The First Project of the World Climate Research Program', *Bull. Amer. Meteor. Soc.* **64**, 779–784.

Schiffer, R. A. and Rossow, W. B.: 1985, 'ISCCP Global Radiance Data Set: A New Resource for Climate Research', *Bull. Amer. Meteor. Soc.* **66**, 1498–1505.

Schlesinger, M. E. and Mitchell, J. F. B.: 1985, 'Model Projections of the Equilibrium Climatic Response to Increased Carbon Dioxide', in M. C. MacCracken and F.M. Luther, (eds.), *The Potential Climatic Effects of Increasing Carbon Dioxide,* DOE/ER–0237, 81–148.

Schneider, S. H.: 1972, 'Cloudiness as a Global Climatic Feedback Mechanism: The Effect on the Radiation Balance and Surface Temperature of Variations in Cloudiness', *J. Atmos. Sci.* **29**, 1413–1422.

Schneider, S. H.: 1986, 'Can Modeling of the Ancient Past Verify Predictions of Future Climate?-An editorial', *Clim. Change* **8**, 117–120.

Shukla J. and Sud, Y.: 1981, 'Effect of Cloud Radiation Feedback on the Climate of a General Circulation Model', *J. Atmos. Sci.* **38**, 2339–2353.

Somerville, R. C. and Remer, L. A.: 1984, 'Cloud Optical Thickness Feedbacks in the CO_2-Climate Problem', *J. Geophys. Res.* **89**, 9668–9672.

Stephens, G. L. and Webster, P. J.: 1979, 'Sensitivity of Radiative Forcing to Variable Cloud and Moisture', *J. Atmos. Sci.* **36**, 1542–1556.

Stowe. L. L.: 1984, 'Evaluation of Nimbus 7 THIR/CLE and Air Force Three-Dimensional Nephanalysis Estimates of Cloud Amount', *J. Geophys. Res.* **89**, 5370–5380.

Van Loon, H., Taljaard, J. J., Sasamori, T., London, J., Hoyt, D. V. Labicze, K., and Newton, C. W.: 1972, *Meteorology of the Southern Hemisphere, Meteorol. Monogr.* **13**, Amer. Meteor. Soc., Boston, Mass.

Wang, W. -C., Rossow, W. B., Yao, M. -S., and Wolfson, M.: 1981, 'Climate Sensitivity of a One-Dimensional Radiative-Convective Model with Cloud Feedback, *J. Atmos. Sci.*, **38**, 1167–1178.

Warren, S. G. and Schneider, S. H.: 1979, 'Seasonal Simulation as a Test for Uncertainties in the Parameterizations of a Budyko-Sellers Zonal Climate Model', *J. Atmos. Sci.* **36**, 1377–1391.

Warren, S. G., Hahn, C. J., and London, J.: 1985, 'Simultaneous Occurrence of Different Cloud Types', *J. Clim. Appl. Meteor.* **24**, 658–667.

Washington, W. M. and Meehl, G. A.: 1984, 'Seasonal Cycle Experiment on the Climate Sensitivity Due to a Doubling of CO_2 with an Atmospheric General Circulation Model Coupled to a Simple Mixed-layer Ocean Model', *J. Geophys. Res.* **89**, 9475–9503.

Webster, P. J. and Stephens, G. L.: 1984, 'Cloud-Radiation Interaction and the Climate Problem', in J. T. Houghton (ed.), *The Global Climate*, C.U.P., Cambridge, pp. 63–78.

Wetherald, R. T. and Manabe, S: 1980, 'Cloud Cover and Climate Sensitivity', *J. Atmos. Sci.* **37**, 1485–1510.

Wetherald, R. T. and Manabe, S.: 1986, 'An Investigation of Cloud Cover Change in Response to Thermal Forcing', *Climatic Change* **8**, 5–23.

Wigley, T. M. L.: 1982, 'Energy Production and Climatic Change: An Assessment', *Uranium and Nuclear Energy: 1981. Proc. Sixth Int. Symp.*, Uranium Institute, Butterworth Scientific, pp. 289–322.

Wigley, T. M. L.: 1983, 'The Pre-Industrial Carbon Dioxide Level', *Climatic Change* **5**, 315–320.

Wigley, T. M. L. and Schlesinger, M. E.: 1985, 'Analytical Solution for the Effect of Increasing CO_2 on Global Mean Temperature', *Nature* **315**, 649–652.

Wigley, T. M. L., Jones, P. D., and Kelly, P. M., 1980, 'Scenario for a Warm, High-CO_2 World', *Nature* **283**, 17–21.

Wilson, C. A. and Mitchell, J. F. B.: 1986, 'Diurnal Variation and Cloud in a General Circulation Model', *Quart. J. Roy. Meteor. Soc.* **112**, 347–369.

WMO: 1986, Report of the International Conference on the assessment of the Role of Carbon Dioxide and of Other Greenhouse Gases in Climate Variations and Associated Impacts, held in Villach, Austria (October, 1985), WMO No. 661, World Meteorological Organization, Geneva, Switzerland, 78 pp.

(Received 23 December, 1985; in revised form 25 July, 1986).